

St. John Fisher University

Fisher Digital Publications

Pharmacy Faculty/Staff Publications

Wegmans School of Pharmacy

12-8-2016

Formulation and characterization of an apigenin-phospholipid phytosome (APLC) for improved solubility, in vivo bioavailability, and antioxidant potential

Darshan R. Telange
Nagpur University


Arun T. Patin
Nagpur University

Anil M. Pethe
SVKM's NMIMS University

Harshal Fegade
Nagpur University

Sridhar Anand
St. John Fisher University, sanand@sjf.edu

Follow this and additional works at: https://fisherpub.sjf.edu/pharmacy_facpub

 *next page for additional authors*

 Part of the [Pharmacy and Pharmaceutical Sciences Commons](#)

Publication Information

Telange, Darshan R.; Patin, Arun T.; Pethe, Anil M.; Fegade, Harshal; Anand, Sridhar; and Dave, Vivek S. (2016). "Formulation and characterization of an apigenin-phospholipid phytosome (APLC) for improved solubility, in vivo bioavailability, and antioxidant potential." *European Journal of Pharmaceutical Sciences* 108, 36-49.

Please note that the Publication Information provides general citation information and may not be appropriate for your discipline. To receive help in creating a citation based on your discipline, please visit <http://libguides.sjfc.edu/citations>.

This document is posted at https://fisherpub.sjf.edu/pharmacy_facpub/117 and is brought to you for free and open access by Fisher Digital Publications at . For more information, please contact fisherpub@sjf.edu.

Formulation and characterization of an apigenin-phospholipid phytosome (APLC) for improved solubility, *in vivo* bioavailability, and antioxidant potential

Abstract

The apigenin-phospholipid phytosome (APLC) was developed to improve the aqueous solubility, dissolution, *in vivo* bioavailability, and antioxidant activity of apigenin. The APLC synthesis was guided by a full factorial design strategy, incorporating specific formulation and process variables to deliver an optimized product. The design-optimized formulation was assayed for aqueous solubility, *in vitro* dissolution, pharmacokinetics, and antioxidant activity. The pharmacological evaluation was carried out by assessing its effects on carbon tetrachloride-induced elevation of liver function marker enzymes in a rat model. The antioxidant activity was assessed by studying its effects on the liver antioxidant marker enzymes. The developed model was validated using the design-optimized levels of formulation and process variables. The physical-chemical characterization confirmed the formation of phytosomes. The optimized formulation demonstrated over 36-fold higher aqueous solubility of apigenin, compared to that of pure apigenin. The formulation also exhibited a significantly higher rate and extent of apigenin release in dissolution studies. The pharmacokinetic analysis revealed a significant enhancement in the oral bioavailability of apigenin from the prepared formulation, compared to pure apigenin. The liver function tests indicated that the prepared phytosome showed a significantly improved restoration of all carbon tetrachloride-elevated rat liver function marker enzymes. The prepared formulation also exhibited antioxidant potential by significantly increasing the levels of glutathione, superoxide dismutase, catalase, and decreasing the levels of lipid peroxidase. The study shows that phospholipid-based phytosome is a promising and viable strategy for improving the delivery of apigenin and similar phytoconstituents with low aqueous solubility.

Keywords

fsc2017

Disciplines

Pharmacy and Pharmaceutical Sciences

Comments

This is the authors' accepted manuscript version of the article. The final published article is available on the publisher's webpage: <http://doi.org/10.1016/j.ejps.2016.12.009>

Creative Commons License



This work is licensed under a [Creative Commons Attribution-NonCommercial-No Derivative Works 4.0 International License](https://creativecommons.org/licenses/by-nc-nd/4.0/).

Authors

Darshan R. Telange, Arun T. Patin, Anil M. Pethe, Harshal Fegade, Sridhar Anand, and Vivek S. Dave

Formulation and characterization of an Apigenin-Phospholipid Phytosome (APLC) for improved solubility, *in vivo* bioavailability, and antioxidant potential

Darshan R. Telange¹, Arun T. Patil¹, Anil M. Pethe², Harshal Fegade¹, Sridhar Anand³, Vivek S. Dave^{3*}

¹Department of Pharmaceutical Sciences, R.T.M. Nagpur University, Nagpur, Maharashtra, India

²SPP School of Pharmacy & Technology Management, Pharmaceutics Division, SVKM's NMIMS University, Mumbai, Maharashtra, India

³St. John Fisher College, Wegmans School of Pharmacy, Rochester, NY, USA

**Corresponding author*

Vivek S. Dave, Ph.D.

St. John Fisher College

Wegmans School of Pharmacy

Rochester, NY, 14534

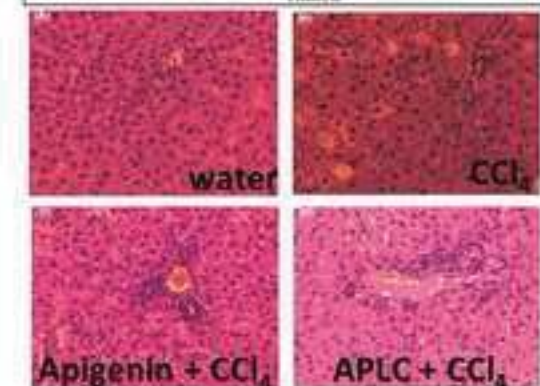
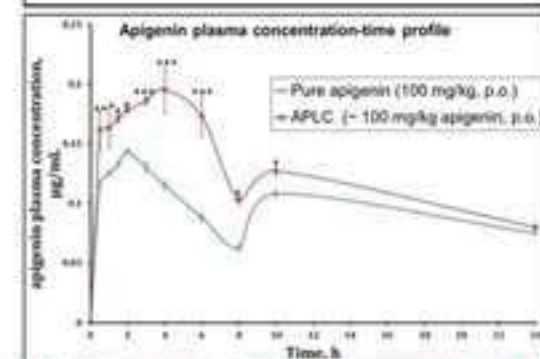
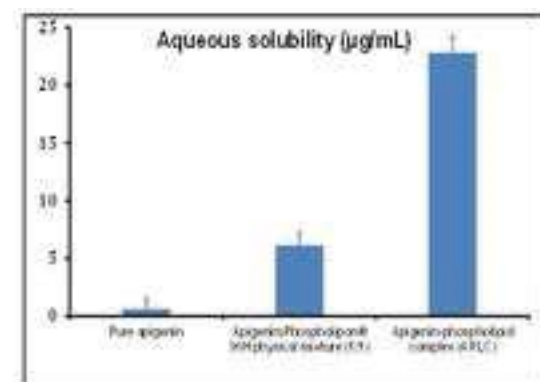
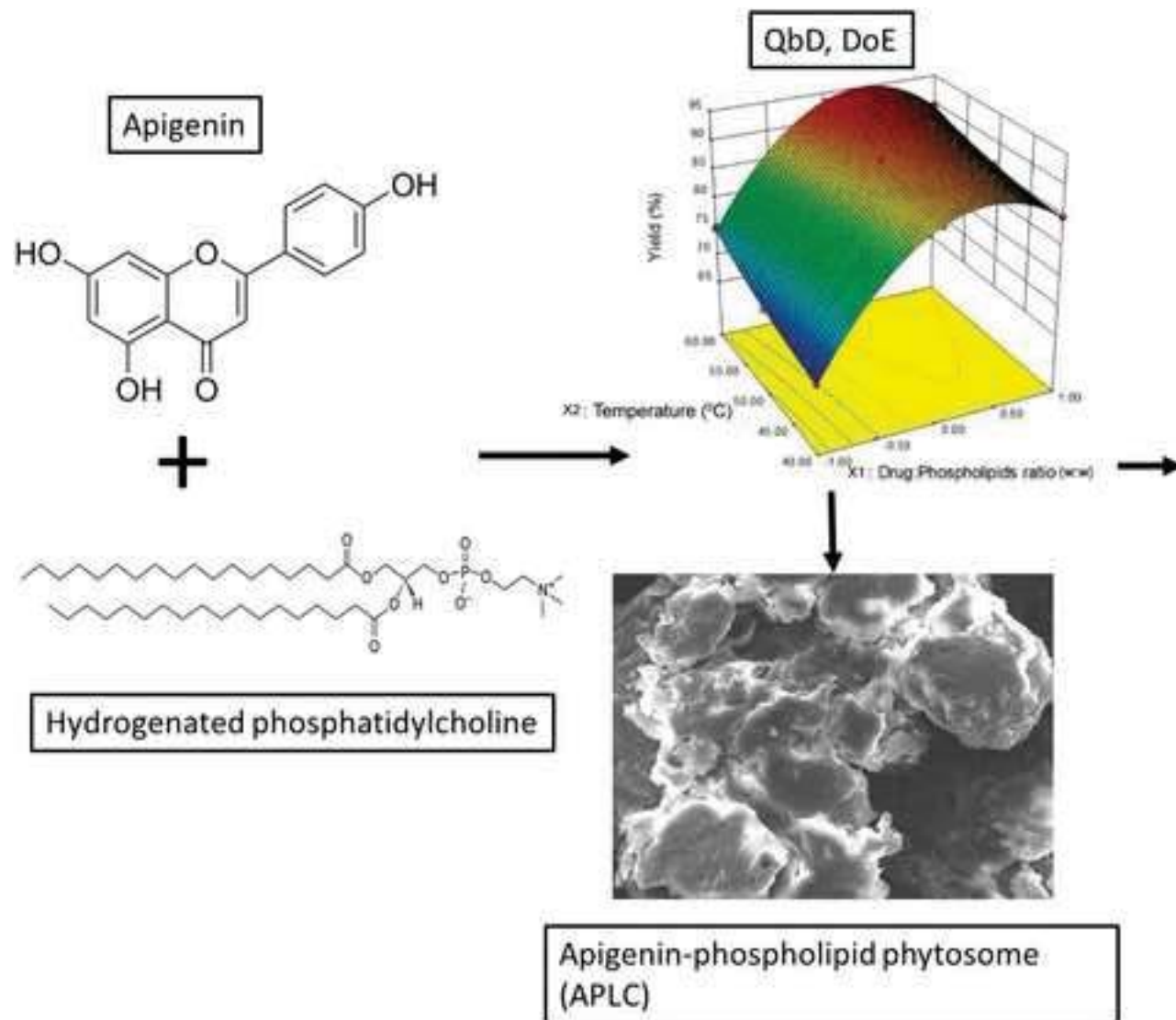
Ph. 1-585-385-5297

Fax. 1-585-385-5295

E-mail: vdave@sjfc.edu

Abstract

The apigenin-phospholipid phytosome (APLC) was developed to improve the aqueous solubility, dissolution, *in vivo* bioavailability, and antioxidant activity of apigenin. The APLC synthesis was guided by a full factorial design strategy, incorporating specific formulation and process variables to deliver an optimized product. The design-optimized formulation was assayed for aqueous solubility, *in vitro* dissolution, pharmacokinetics, and antioxidant activity. The pharmacological evaluation was carried out by assessing its effects on carbon tetrachloride-induced elevation of liver function marker enzymes in a rat model. The antioxidant activity was assessed by studying its effects on the liver antioxidant marker enzymes. The developed model was validated using the design-optimized levels of formulation and process variables. The physical-chemical characterization confirmed the formation of Phytosomes. The optimized formulation demonstrated over 36-fold higher aqueous solubility of apigenin, compared to that of pure apigenin. The formulation also exhibited a significantly higher rate and extent of apigenin release in dissolution studies. The pharmacokinetic analysis revealed a significant enhancement in the oral bioavailability of apigenin from the prepared formulation, compared to pure apigenin. The liver function tests indicated that the prepared phytosome showed a significantly improved restoration of all carbon tetrachloride-elevated rat liver function marker enzymes. The prepared formulation also exhibited antioxidant potential by significantly increasing the levels of glutathione, superoxide dismutase, catalase, and decreasing the levels of lipid peroxidase. The study shows that phospholipid-based phytosome is a promising and viable strategy for improving the delivery of apigenin and similar phytoconstituents with low aqueous solubility.



1. Introduction

Apigenin is a hydrophobic, polyphenolic flavonoid compound commonly found in fruits, vegetables, tea, chamomile, wheat sprouts etc. (Shukla and Gupta, 2010). Apigenin-containing preparations are marketed as dietary and herbal supplements (Peterson and Dwyer, 1998). It has been demonstrated to possess anti-oxidant (Prince Vijeya Singh et al., 2004; Stanojević et al., 2009), anti-microbial (Taleb-Contini et al., 2003), anti-inflammatory (Funakoshi-Tago et al., 2011; Rithidech et al., 2012), anti-proliferative (Johnson and Gonzalez de Mejia, 2013), anti-viral (Shibata et al., 2014), antidiabetic (Choi et al., 2014), and tumor inhibitory activities (Choudhury et al., 2013; Ruela-de-Sousa et al., 2010).

The clinical potential of apigenin is stifled by its poor aqueous solubility, rapid metabolism, and low oral bioavailability. Apigenin has an aqueous solubility of less than 2.16 µg/mL, and rated as a Class II drug, based on the Biopharmaceutics Classification System (BCS) (Zhang et al., 2012). After oral administration in rats, apigenin undergoes rapid metabolism to key metabolites, such as *p*-hydroxy phenyl propionic acid, *p*-hydroxy cinnamic acid, and *p*-hydroxy benzoic acid (Griffiths and Smith, 1972). Furthermore, it demonstrated only 51% bioavailability after oral administration of *Flos chrysanthemi* extract (100 mg/kg) in rats (Chen et al., 2012). Thus, it is necessary to overcome these limitations using novel formulation strategies to improve apigenin delivery.

Several formulation strategies and techniques e.g. liposomes (Arsić et al., 2011), nanocrystal gel formulations (Al Shaal et al., 2011), and self-micro emulsifying drug delivery systems (SMEDDS) (Zhao et al., 2013) have been investigated to improve the delivery of apigenin. Munyendo *et al* reported that the formulation of *D*- α -tocopherol acid and polyethylene glycol 1000 succinate (TPGS) stabilized the mixed micelles of apigenin and phospholipids in their

evaluation anticancer properties (Munyendo et al., 2013). Karthivashan *et al* prepared ‘flavonosomes’ (phytosomes loaded with multiple flavonoids) using phosphatidylcholine as a carrier, and evaluated their *in vitro* pharmacokinetics and toxicity (Karthivashan et al., 2016). Shen *et al* evaluated a novel topical delivery system for apigenin by using soy lecithin-based ethosomes (Shen et al., 2014). The authors demonstrated a superior skin targeting with the prepared ethosomes. Additionally, apigenin-loaded ethosomes also showed a significant reduction of cyclooxygenase-2 levels in mouse skin inflammation induced by ultraviolet B (UVB) light. Pawlikowska-Pawlega *et al* studied the interaction of apigenin within liposomes formed with dipalmitoylphosphatidylcholine (DPPC) using FTIR spectroscopy, ¹H-NMR, and EPR techniques, and also investigated its chemopreventive activity via changing the fluidity of tumor cell membranes (Pawlikowska-Pawlega et al., 2013).

While these formulation methods were shown to improve the solubility, dissolution, or *in vitro* activity of apigenin, a systematic evaluation of the bioavailability and *in vivo* pharmacokinetics of apigenin is missing in literature; this is particularly true for oral administration of apigenin, or novel formulations of apigenin.

Semalty *et al* reviewed the potential benefits of pharmacosomes, novel lipid-based drug delivery systems, in improving the biopharmaceutical properties of several drugs (Semalty et al., 2009). Previous studies have demonstrated that an appropriate carrier system like phospholipids can improve the aqueous solubility, permeability, and overall bioavailability of such compounds. The studies with *Centella asiatica* (Saoji et al., 2016), matrine (Ruan et al., 2010), oxymatrine (Yue et al., 2010), curcumin (Zhang et al., 2013), catechin (Semalty et al., 2012), chrysophanol (Singh et al., 2012), naringenin (Semalty et al., 2014) have shown that molecular aggregation with phospholipids increased their oral bioavailability by improving the aqueous solubility,

permeability, and other properties of these phytochemicals. Semalty *et al* discussed the usefulness of supramolecular phospholipids–polyphenolics adducts (PHYTOSOME[®]) in improving the solubility and permeability of low water-soluble polyphenolic compounds across a broad pharmacological spectrum (Semalty et al., 2010). In a recent review, Semalty A. provided a comprehensive analysis of cyclodextrin-, and phospholipid-based aggregates in the enhancement of solubility, dissolution, and overall bioavailability of Biopharmaceutical Classification System (BCS) Class II and Class IV drugs (Semalty, 2014).

The present work aims to formulate, optimize, characterize an apigenin–phospholipid phytosome (APLC), and evaluate the optimized formulation for both enhanced aqueous solubility and oral bioavailability of apigenin in a rat model. Additionally, a preliminary pharmacological analysis was carried out to evaluate the *in vivo* antioxidant potential after oral administration of APLC in rats.

2. Materials and Methods

2.1. Materials

Apigenin was obtained from Shandong Northwest Manufacturing Co., China. Phospholipon[®] 90H was obtained from Lipoid GmbH, Ludwigshafen, Germany. 1, 4 – dioxane, 2, 2-diphenyl-1-picrylhydrazyl (DPPH), 5,5'-dithiobis-2-nitrobenzoic acid (DTNB, Ellman's Reagent), and 3-(2-Pyridyl)-5,6-diphenyl-1,2,4-triazine-*p,p'*-disulfonic acid monosodium salt hydrate (FerroZine[™] Iron Reagent) were obtained from Loba Chemie Pvt. Ltd., Mumbai, India. *n*-hexane, *n*-octanol, thiobarbituric acid, and trichloroacetic acid were purchased from Sigma-Aldrich Corporation, St. Louis, MO. All other chemicals used were of analytical grade.

2.2. Formulation of apigenin-phospholipid phytosome

The APLC was prepared using different molar ratios of (1:1, 1:2 and 1:3) based on earlier reported techniques (Bhattacharyya et al., 2014; Maiti et al., 2007). Briefly, accurately weighed amounts of apigenin and phospholipid were placed into a 100 mL round bottom flask, and dissolved in 20 mL of a mixture of 1, 4-dioxane:methanol (14:6). The reaction temperature of the reflux was controlled at 40 °C, 50 °C, or 60 °C using a water bath for two h. The flask contents were then concentrated to obtain a dry residue. This dried material was dissolved in a 50 mL mixture of chloroform: methanol (45:5). The solution was then concentrated to 2-3 mL and poured into 100 mL of *n*-hexane. The resulting APLC was precipitated and filtered. Subsequently, the phytosome was dried completely under vacuum at 40 °C. The dried APLC (yield ~90% w/w) was transferred to a light-protected (amber) glass vial purged with nitrogen, and stored at room temperature.

2.3. The extent of Apigenin incorporation in the prepared APLC (% yield)

An accurately weighed amount of APLC (equivalent to 10 mg of apigenin) was added to 5 mL of chloroform. The formed phytosome and the unreacted phospholipid dissolves in chloroform, but the free (non-aggregated) apigenin remains practically insoluble in chloroform (Tan et al., 2012). The dispersion was filtered and the free or non-aggregated apigenin was separated as a precipitate. This non-aggregated apigenin was dissolved in methanol and assayed using a UV-visible spectrophotometer (Model: V-630, JASCO International Co. Ltd., Tokyo, Japan) at 335 nm for apigenin.

2.4. Full-factorial design (3²)

A full factorial design was adopted to study the overall influence of specific independent variables, *viz.*, drug: phospholipids ratio (X_1 , w: w), and temperature (X_2 , °C) on the extent of

apigenin incorporation (% yield). The two independent variables (X_1 and X_2) were selected at three levels, coded as -1 (low), 0 (middle), and +1 (higher), resulting in a 3^2 factorial design of nine possible combinations. The extent of apigenin incorporation (% yield) was defined as the dependent variable. The experimental trials were performed using all nine possible combinations of the selected variables. The mathematical model containing coefficient effects, interactions, and polynomial terms was analyzed to assess the response using the following equation:

$$Y = b + b_1X_1 + b_2X_2 + b_3X_{12} + b_4X_{22} + b_5X_1X_2$$

where Y is the dependent variable, b is the coefficient of the independent variable X . The main effects (X_1 and X_2) represent the possible aggregate effect of both factors as they change independently from their low to high level. The interaction term (X_1X_2) shows how the response changes when two factors are simultaneously changed. The polynomial terms (X_{12} and X_{22}) describes the non-linearity. The design levels and the real values of the independent variables are shown in Table 1. The composition of experimental trials along with obtained yield (%) values are shown in the Table 2.

2.5. Physicochemical characterization

2.5.1. Particle size analysis and zeta potential

Photon Cross-Correlation Spectroscopy (PCCS) with dynamic light scattering was used to analyze the particle size distribution of the prepared APLC. Briefly, about 5 mg of APLC powder was dispersed in 10 mL deionized water in a sample vial. The sample vial was inserted manually into the sample chamber of the analyzer (Model: NANOPHOX, Sympatec GmbH, Clausthal-Zellerfeld, Germany) with a sensitivity range of 1 nm to 10 μ m. The count rate was optimized by selecting an appropriate position of the sample vial with the help of the associated software. All measurements were carried out at a fixed temperature of 25 °C.

The zeta potential of the APLC powder was measured using a Dynamic Light Scattering (DLS) zeta potential and nano particle analyzer (Model: NanoPlusTM-2, Particulate Systems, Norcross, GA, USA) with a zeta potential range of -200 to +200 mV.

2.5.2. Differential scanning calorimetry (DSC)

The samples of pure apigenin, pure Phospholipon[®] 90H, the physical mixture (PM) of apigenin and Phospholipon[®] 90H, and the APLC were analyzed for their thermal behavior using a differential scanning calorimeter (Model: DSC-1 821e, Mettler-Toledo AG, Analytical, Schwerzenbach, Switzerland). Dried nitrogen (50 mL/min) was used as a purge gas. The instrument was calibrated for the heat flow and heat capacity with high-purity indium standard using standard procedures reported elsewhere. Each sample (2.0 ± 0.2 mg) followed a single heating cycle with temperature ramping from 40 °C to 400 °C at a heating rate of 10 °C min⁻¹. The analysis of the event peaks for all the samples was carried out using the software accompanying the instrument.

2.5.3. Fourier transform infrared spectroscopy (FTIR)

The molecular interactions between the formulation components were analyzed by obtaining the infrared scans of pure apigenin, Phospholipon[®] 90H, PM, and APLC on a FTIR spectrophotometer (Model: FTIR-8300, Shimadzu Corporation, Kyoto, Japan). Briefly, individual samples (~2 mg) were uniformly mixed with potassium bromide (KBR, ~200mg) and compressed under pressure of 10 Ton/nm² to prepare circular transparent discs. The samples were previously dried in a hot air oven at 50 °C for 2 h to theoretically remove the influence of residual moisture, if any. Each analysis included 45 scans, at a resolution of 4 cm⁻¹ in the wavelength range 4000 to 400 cm⁻¹. The data was analyzed using IRsolution FTIR control software (version: 1.10) associated with the instrument.

2.5.4. Proton nuclear magnetic resonance (¹H-NMR)

The proton nuclear magnetic resonance (¹H-NMR) spectra of pure apigenin, pure Phospholipon[®] 90H, PM, and APLC were obtained on a 400 MHz FT-NMR spectrophotometer (Bruker Avance II, Bruker BioSpin, Billerica, MA) with a temperature range of -90 °C to 80 °C . All samples were analyzed at 292 K (18.85 °C).

2.5.5. Powder x-ray diffractometry (PXRD)

The samples of pure apigenin, Phospholipon[®] 90H, PM, and APLC were analyzed for their polymorphic state by obtaining their x-ray diffraction scans. This was done using a powder x-ray diffractometer (Model: D8 ADVANCE, Bruker AXS, Inc., Madison, WI, USA) operating with a Bragg-Brentano geometry ($\theta/2\theta$) optical setup. Briefly, the samples were mounted uniformly as a thin layer on the sample holder. A one dimensional detector (LYNXEYE[™]) for x-ray diffraction, based on Bruker AXS' compound silicon strip technology was used to monitor diffraction. The samples were irradiated with a monochromatic CuK β radiation ($\lambda=1.5406\text{\AA}$) at an operating voltage and amperage of 30 mV and 10 mA, respectively. The samples were scanned with the diffraction angle increasing from 3° to 60°, 2θ angle, with a step-angle of 0.04° 2θ and a count time of 5 seconds. The angular spin for the samples was $\Phi = 360^\circ$.

2.5.6. Solubility analysis

The aqueous solubilities of pure apigenin and apigenin in the prepared APLC were determined by a method similar to that described earlier (Saoji et al., 2016). Briefly, an excess of apigenin or APLC were added to 5 mL of water or *n*-octanol in sealed glass containers at room temperature (25 °C). The liquid was agitated for 24 h, followed by centrifugation for 25 min at 1500 rpm. The supernatant was filtered through a membrane filter (0.45 μ). 1 mL of this filtrate, after

appropriate dilutions, was assayed using a UV-visible spectrophotometer (Model: V-630, JASCO International Co. Ltd., Tokyo, Japan) at 335 nm for apigenin.

2.6 Functional characterization

2.6.1 *In vitro* dissolution studies

The *in vitro* dissolution behavior of pure apigenin, and apigenin in the prepared APLC was analyzed using a dialysis method reported earlier (Maiti et al., 2009). Briefly, a dialysis membrane (LA393, Dialysis Membrane-70, Average diameter 17.5 mm, Average flat width 28.46 mm, and capacity ~ 2.41 mL/cm; HiMedia Laboratories, Mumbai, India), which retains molecules >12,000 kDa was used to prepare dialysis bags for the samples. The membrane was washed according to the manufacturer guidelines. 2 mL of apigenin suspension (2 mg/mL) or APLC (~4 mg apigenin) was added to dialysis bag and tied. The tied membrane bag was suspended into a beaker containing phosphate buffer saline (PBS, 200 mL, pH 7.4) with (Tween[®] 20, 1% w/v). The contents of the beakers were stirred at 50 rpm using a magnetic stirrer at $37 \pm 1^\circ\text{C}$. At predetermined intervals, 5 mL aliquots were withdrawn and assayed using a UV-visible spectrophotometer (Model: V-630, JASCO International Co. Ltd., Tokyo, Japan) at 335nm to estimate the release of apigenin.

2.6.2 *In vivo* antioxidant activity

The influence of pure apigenin, and the prepared APLC on the liver function test, and their *in vivo* antioxidant activity was evaluated using the method previously reported in literature (Maiti et al., 2007; Maiti et al., 2009).

2.6.2.1 *Animals*

Male and female albino rats (Wistar strain, bred in-house, 150-200 g) were employed for the evaluation of *in vivo* antioxidant activity of pure apigenin and APLC. All animals were housed in colony cages in groups of four at controlled temperature ($25 \pm 5^\circ\text{C}$) and humidity ($50 \pm 5\% \text{RH}$)

conditions, with a 12 h light/dark cycle. The food (pellet chow, Brooke Bond, Lipton, India) and water were provided *ad libitum*. The experimental protocol (UDPS/IAEC/2013–14/05, dated February 14, 2014) for the study was approved by the Institutional Animal Ethics Committee (IAEC) of the University Department of Pharmaceutical Sciences (UDPS), R. T. M. Nagpur University, Nagpur, India. The experimental protocols were followed according to the ethical guidelines provided by the Committee for the Purpose of Control and Supervision of Experiments on Animals (CPCSEA).

2.6.2.2 Dosing

The animals were divided into four groups, with six animals in each group. Group I and Group II animals received Tween[®] 20 (1% v/v, p.o.) diluted with distilled water for seven days. On the seventh day, Group II animals received a single dose of a mixture of CCl₄ and olive oil (1:1, 5 mL/kg, i.p.). Group I served as negative control and Group II served as the positive control. Group III animals received pure apigenin (25 mg/kg, p.o.) suspension in distilled water with Tween[®] 20 (1% v/v) for seven days. On the seventh day, this group also received a single dose of a mixture of CCl₄ and olive oil (1:1, 5 mL/kg, i.p.). Group IV animals received APLC (~25 mg/kg apigenin, p.o.) for seven days. On the seventh day, this group also received a single dose of a mixture of CCl₄ and olive oil (1:1, 5 mL/kg, i.p.). After 24 h of CCl₄ administration, all the animals were anaesthetized using ether. The blood samples of all animals were collected from the retro orbital plexus and centrifuged. The animals were subsequently euthanized by cervical decapitation. The supernatant plasma samples were used for the liver function test. Additionally, the livers of all animals were dissected immediately and washed in ice cold saline. The livers were homogenized in 0.1 M phosphate buffer saline (PBS, pH 7.4) and centrifuged to obtain a clear supernatant. This solution was used to estimate the *in vivo* antioxidant marker enzymes.

2.6.2.3 Liver marker enzyme estimation (liver function test)

The influence of pure apigenin and APLC on rat liver function was evaluated by quantitative determination of serum glutamic oxaloacetic transaminase (SGOT), serum glutamic pyruvic transaminase (SGPT), serum alkaline phosphatase (SALP), and total bilirubin. A method previously described in literature was used to estimate SGOT and SGPT levels (Reitman and Frankel, 1957). Briefly, 0.5 mL of substrate [α -L-alanine (200 mM) for SGOT, or L-aspartate (200 mM) with 2 mM α -ketoglutarate for SGPT] was incubated for 5 min at 37 °C. 0.1 mL rat plasma was added to the substrate and the volume was adjusted to 1 mL with sodium phosphate buffer (pH 7.4, 0.1 M). The mixture was incubated for either 30 min (SGPT) or 60 min (SGOT). 2, 4-dinitrophenylhydrazine (DNPH, 0.5 mL, 1 mM) was then added to this reaction mixture and left for additional 30 min at room temperature. Finally, 5 mL sodium hydroxide (NaOH, 0.4 N) was added to the mixture and the resultant solution was analyzed by colorimetry at 505 nm.

SALP levels were estimated using a method previously described by Kind et al. (Kind and King, 1954). Briefly, 1 mL of substrate was incubated in 1 mL sodium bicarbonate buffer for 3 min at 37 °C. To this solution, 100 μ L plasma was added, vortexed, and incubated again for 15 min at 37 °C. After incubation, 0.8 mL sodium hydroxide (0.5 N), 1.2 mL of sodium bicarbonate (0.5 N), 1 mL aminoantipyrine (0.6% w/v), and 1 mL potassium ferricyanide were added and mixed well. The absorbance of the resulting mixture was measured at 520 nm.

The total bilirubin in plasma was quantified using the method reported by Malloy et al. (Malloy and Evelyn, 1937). Briefly, 5 mL of sulfanilic acid solution (4 mmol/L) was added to 0.1 mL of sodium nitrite solution (144 mmol/L). To this solution, 0.25 mL plasma was added. The mixture was incubated for 10 min at 37 °C and the absorbance measured at 670 nm.

2.6.2.4 In vivo antioxidant marker enzyme estimation

The antioxidant potential of pure apigenin and APLC was assessed by the quantitative estimation of glutathione (GSH), superoxide dismutase (SOD), catalase (CAT), and lipid peroxidase (LPO). GSH in rat liver homogenate was estimated using a previously reported method by Ellman (Ellman, 1959). First, a precipitating mixture was prepared by dissolving 1.67 g metaphosphoric acid, 0.2 g EDTA, and 30 g NaCl in distilled water to make up 100 mL aqueous solution. Following the Ellman protocol, 0.2 mL rat liver homogenate, 1.8 mL distilled water, and 0.3 mL precipitating mixture were combined and centrifuged at 5000 rpm for 5 min to separate proteins. To 1 mL of the supernatant, 1.5 mL phosphate buffer (0.1 M) and 0.5 mL DTNB reagent were added. The contents was mixed in a vial and the absorbance of the solution was measured at 412 nm using UV-visible spectrophotometer (Model: V-630, JASCO International Co. Ltd., Tokyo, Japan). The concentration of GSH was expressed as $\mu\text{g}/\text{mg}$ of protein.

A method described by Marklund et al. was used to quantitatively estimate SOD in rat liver homogenate (Marklund and Marklund, 1974). Briefly, a reaction mixture was prepared by the addition of 2 mL Tris-HCl buffer (75 mM, pH 8.2), 0.6 mL EDTA (6 mM), 20 μL rat liver homogenate, and 0.5 mL freshly prepared pyrogallol solution (30 mM). An increase in absorbance and change in absorbance/min for the resulting solution was measured against blank for 3 min at 30 second intervals at 420 nm using UV-visible spectrophotometer (Model: V-630, JASCO International Co. Ltd., Tokyo, Japan). One unit of enzyme activity is considered equivalent to 50% inhibition in the rate of auto-oxidation of pyrogallol. The activity of SOD was expressed as units/mg of protein.

Lipid peroxidase (LPO) in rat liver homogenate was estimated using the method of Stocks et al. (Stocks and Dormandy, 1971). To a vial, 0.5 mL rat liver homogenate, 0.2 mL

sodium lauryl sulfate (8.1% w/v), 1 mL trichloroacetic acid (20% w/v), and 1.5 mL thiobarbituric acid (0.8%, w/v) were mixed. This mixture was heated at 100 °C for 1 h. The mixture was then allowed to cool to room temperature (25 °C) and 1 mL of distilled water was added. Centrifugation of the mixture at 4000 rpm for 10 min helped separate the organic layer. The absorbance of organic layer was measured at 532 nm using UV–visible spectrophotometer (Model: V-630, JASCO International Co. Ltd., Tokyo, Japan). The lipid peroxidation was calculated on the basis of the molar extinction coefficient of malondialdehyde (MDA) ($1.56 \times 10^5 \text{ M}^{-1} \text{ cm}^{-1}$), and presented in terms of MDA (nM/g) in hemoglobin.

CAT was quantitatively estimated using the method reported by Beers et al. (Beers and Sizer, 1952). Briefly, in a cuvette, 0.1 mL rat liver homogenate and 1.9 mL phosphate buffer (50 mM, pH 7.4) were added. The reaction was initiated by the addition of 1.0 mL of freshly prepared hydrogen peroxide (H_2O_2 , 30 mM). The decomposition rate of H_2O_2 was measured at 240 nm using a UV–visible spectrophotometer (Model: V-630, JASCO International Co. Ltd., Tokyo, Japan).

2.6.2.5 Histopathological studies

At the end of the treatment period, animals from all four treatment groups were euthanized and their livers dissected. The isolated livers were maintained in a buffered formalin (10% v/v) solution. The livers were then carefully sectioned and stained with hematoxylin and eosin reagent. The liver sections were examined under an optical microscope (Model: DM2500, Leica Microsystems Inc., Buffalo Grove, IL). The images were captured at a magnification of 400× with the attached digital camera.

2.6.3 Oral bioavailability studies

2.6.3.1 LC-MS/MS analysis method

A LC-MS/MS analytical method previously reported in the literature was followed for the quantitative evaluation of samples (Duan et al., 2011). The instrument employed for the study was a triple quadrupole mass spectrometer (Model: Thermo Scientific™ TSQ Quantum™ Access MAX, Thermo Fisher Scientific Inc., Waltham, MA, USA), equipped with an online degasser, column heater, and an auto sampler. The stationary phase consisted of a C₁₈ HPLC column (100 mm x 4.6 mm, Thermo Scientific™ Hypersil GOLD™, Thermo Fisher Scientific Inc., Waltham, MA, USA) with a particle size of 5 µm and maintained at 25 °C. The mobile phase consisted of methanol with formic acid (0.1% v/v) and the flow rate was fixed at 1.5 mL/min. To achieve the best possible resolution of apigenin peaks, the method was standardized using quercetin as the internal standard. Chromatographic peaks were detected at 360 nm for quantitative analysis. The mass spectrometric analysis of the samples was carried out in a positive ionization mode using the selected reaction monitoring (SRM). The ion source temperature was 500 °C. The target ions were monitored at *m/z* of 271.22 for apigenin and 303.01 for quercetin. The data acquisition, peak integration, and other analysis was performed using the associated software (Thermo Scientific™ LCQUAN™, version 2.6, Thermo Fisher Scientific Inc., Waltham, MA, USA).

2.6.3.2 Extraction of apigenin from plasma and sample preparation

A sample preparation technique previously reported by Chen et al. (Chen et al., 2007) was used for the study. Briefly, the laboratory animals were fasted for 12 h with free access to water. The animals divided into two groups of six animals each. Group I received a single dose of apigenin (100 mg/kg, p.o.) and group II received a single dose of APLC (100 mg/kg, p.o.). At

predetermined time intervals, the animals were anesthetized and blood samples obtained from the retro-orbital plexus were collected into Eppendorf® Safe-Lock microcentrifuge tubes (1.5 mL). The blood samples were then centrifuged at 3000 g for 10 min, the plasma separated, collected, and stored at -20 °C prior to analysis.

For the extraction of apigenin from rat plasma, plasma samples (100 µL) were transferred to a test tube and hydrochloric acid (2.0 M) was added to it. The mixture was hydrolyzed at 80 °C for 1.5 h. After allowing to cool to room temperature 1.0 mL ethyl acetate containing quercetin (0.05 µg/mL) was added to this reaction mixture. The mixture was vortexed for 3 min and then centrifuged at 3500 g for 10 min. After centrifugation, 0.8 mL of the supernatant organic phase was transferred to a separate test tube and dried in a vacuum desiccator at room temperature. The dried sample was then reconstituted in the mobile phase (100 µL) and analyzed by the LC-MS/MS method described above.

2.6.3.3 Pharmacokinetic studies

The pharmacokinetic parameters, i.e. maximum plasma concentration (C_{max}) and time to reach maximum concentration (T_{max}), were obtained directly from the concentration–time curve. Other parameters such as half-life ($t_{1/2}$), area under the plasma concentration-time curve from zero to the time of the final measured sample (AUC_{0-t}), area under the plasma concentration-time curve from zero to infinity ($AUC_{0-\infty}$), clearance (cl/F) and volume of distribution (V_z/F), and the relative bioavailability (F) were calculated using a statistical software (WinNonlin®, Version 4.1, Certara USA Inc., Princeton, NJ, USA).

2.7 Statistical analysis

The aqueous solubility and *in vitro* results are presented as mean ± standard deviation. The results from the liver function test, *in vivo* antioxidant activity, and the pharmacokinetic analysis

are presented as mean \pm standard error of mean. The statistical analysis was carried out using one-way analysis of variance (ANOVA) followed by Dunnett's and Student's t-test. *p* values < 0.05 were assumed as statistically significant.

3 Results and discussion

3.1 Formulation of apigenin-phospholipids molecular aggregates (Phytosome)

Flavonoids are generally lipophilic molecules and easily soluble in organic solvents (Jabbari and Gharib, 2012). This physical property is exploited in the current study using the solvent evaporation method to create a stable phytosome of the flavonoid molecule with phospholipids. Existing literature on flavonoids describe the creation of flavonoid-phospholipid aggregates using dichloromethane (DCM) in the solvent evaporation method (Bhattacharyya et al., 2014). However, we found that apigenin possesses poor solubility in DCM resulting in the precipitation of the APLC from DCM. Therefore, the solubility of apigenin and the extent of apigenin incorporation was assessed using other solvents. 1, 4-dioxane is an aprotic solvent with low dielectric constant, and may assist in solubilization of apigenin and phospholipids to result in the formation of stable APLC. We found the binary solvent combination of 1, 4-dioxane: methanol (14:6) to be an optimal solvent system for preparing the APLC. **Note: The solvent, 1, 4-dioxane is used in this study solely for technical reasons, i.e. solubilizing of the formulation components. Due to the reported toxicity profile of 1, 4-dioxane in humans, it is strongly recommended that alternative solvent be explored for further development and/or commercial manufacture of pharmaceutical formulations (Agency for Toxic Substances & Disease Registry, 2012).**

3.2 Full-factorial design (3²)

The results of the extent of apigenin incorporation (% yield) from the experimental trials carried out using a 3² full factorial design are shown in Table 2. The results indicated that the extent of apigenin incorporation was significantly influenced by both the variables studied, i.e. apigenin: phospholipid ratio (X_1 , w:w) and the reaction temperature (X_2 , °C). For the nine experimental batches examined (with different combination of variables), the observed extent of apigenin incorporation ranged between 67 and 94%. These data were used to construct a quadratic model relating the extent of apigenin incorporation (yield, %) to the tested variables. The resulting polynomial equation (Eq. 1, below) was used to draw conclusions based on the magnitude of the coefficient, as well as the sign (+, or -) associated with it.

$$Y = 89.71 + 8.30X_1 + 3.08X_2 + 11.77X_{12} + 0.91X_{22} + 0.75X_1X_2 \quad (1)$$

The estimated coefficient value of b_0 , b_1 , b_2 , and b_3 were found to be statistically significant ($p < 0.05$), whereas b_4 and b_5 were found to be not significant ($p < 0.05$). These observations, coupled with the observed value of the correlation coefficient ($R^2 = 0.9989$), lead us to conclude that this was the best representative model for the study. The positive sign associated with coefficients (b_1 and b_2) indicated a positive correlation between the studied variables and the yield (%). The influence of the studied variables on the yield (%) is also shown in the form of response surface and contour plot (Figure 1). Based on these observations, along with calculations from the developed quadratic model, the optimal values for the studied variables, i.e. drug: phospholipid ratio (X_1 , w:w) and the reaction temperature (X_2 , °C) were found to be 1:2, and 60°C, respectively.

3.3 Validation of the optimized model

An additional batch of APLC was prepared in order to validate the model using the optimized values of the variables,. A comparison between the predicted (theoretical) yield (%) of the APLC obtained from the developed model and the actual yield (%) achieved from the prepared formulation was carried out. The model-predicted value for the average yield (%) of apigenin in the optimized APLC was 93.7%, while the actual yield (%) from the prepared batch was found to be $94.87 \pm 0.93 \%$., indicating both applicability, and validity of the developed model. The bias (%), calculated using the equation (2) below, was also found to be lower than 3% (-1.25%), indicating the relative robustness of the model (Qin et al., 2010).

$$\text{Bias (\%)} = \frac{\text{predicted value} - \text{observed value}}{\text{predicted value}} \times 100 \quad (2)$$

3.4 Physicochemical characterization

3.4.1 Particle size analysis and zeta potential

Particle size and zeta potential are valuable predictors of effective distribution and physical stability of nanoparticles in a liquid medium. According to Tan et al (Tan et al., 2012), the particle size (246.1 nm) of evodiamine–phospholipids complex played a major role in sustained release as well as enhancing oral absorption efficiency of evodiamine. Previously published reports have suggested that lymphatics play a role in the transport of larger particles ($\leq 5 \mu\text{m}$) whereas, endocytosis is a major pathway for the transport of the smaller particles ($\leq 500 \text{ nm}$) (LeFevre et al., 1978; Savic et al., 2003). In the present study, the mean particle size of $107.08 \pm 1.30 \text{ nm}$, with polydispersity index of 0.37 ± 0.012 for APLC is appropriate for oral drug delivery. The low polydispersity index indicates a narrow range of particle size distribution.

Zeta potential (ζ) is a measure of stability of a colloidal dispersion. The zeta potential value ($-22.35 \pm 0.30 \text{ mV}$) obtained for APLC was greater than -30 mV , which indicates excellent

stability of the APLC from flocculation when seen in the context of its low particle size. The zeta potential with range (-20 to 30 mV) was earlier demonstrated as a characteristic property of zeta potential for attraction followed by flocculation exceeding repulsion forces (Dhore et al., 2016; Freitas and Müller, 1998). The zeta potential value depends on the type and composition of phospholipids. In APLC, the low zeta potential value can be elucidated that, the involvement of portion phospholipids with generation of negative charge in aqueous environment with somewhat neutral pH. Hence, with smaller particle size, lower polydispersity index and modest zeta potential value suggested a good physical stability for APLC.

3.4.2 Differential scanning calorimetry (DSC)

Differential scanning calorimetry is a well-established techniques for the analysis of thermal behavior of a wide variety of materials. Measuring changes in material properties as a function of controlled changes in the temperature can provide useful information regarding the melting, degradation, compatibility, stability, and other related properties of test materials. In DSC thermograms these changes exhibit themselves as enthalpy changes, appearance/disappearance of peaks, and changes to a peak's onset time, shape, and relative area. It also provides information of drug-excipient interactions and formation of new entities.

Figure 2 (A, B, C, and D) shows the DSC thermograms of pure apigenin, pure Phospholipon[®] 90H, PM, and APLC, respectively. Pure apigenin (Figure 2A) exhibited a sharp endothermic (melting) peak at 360.82 °C, indicating crystalline nature and purity of apigenin. The thermograms of Phospholipon[®] 90H (Figure 2B) showed two distinct peaks, first peak of lower intensity at 67.16° C and a second relatively sharper peak at 84.83° C. While the intensity of the first peak can be attributed to the melting, the shape of the second peak indicates a phase-transition point. This is suggestive of a change from a gel state to a liquid crystalline state, and

accompanied by isomeric changes to the hydrocarbon segment of the phospholipid, thought to be caused due to movements of the polar segment of phospholipid molecule at increasing temperatures (Li et al., 2013; Yanyu et al., 2006). The thermogram of the physical mixture (PM) (Figure 2C) also shows two dissimilar peaks, i.e. a smaller endothermic peak at 68.34 °C, and a broader peak at 84.84° C. It may be inferred that controlled increase in temperature may cause individual components to melt, and form a partial aggregates *in situ*, whose melting point is lower than apigenin or phospholipid (Ruan et al., 2010). Finally, the thermograms of APLC (Figure 2D) revealed a completely new peak at 75.05° C, and an the original peaks of apigenin and phospholipids appeared to be absent (Galasso et al., 2006). These results are consistent with the previously published reports. Thus, on the basis of comparison of above four DSC thermograms and previous reports it can be concluded that a stable APLC was formed by weak intermolecular interactions (hydrogen bonding, van der Waals interactions, etc.) between apigenin and Phospholipon[®] 90H (Lasonder and Weringa, 1990; Venema and Weringa, 1988; Yanyu et al., 2006). These interactions possibly allow the fatty acid chains of the phospholipid molecule rotate freely and surround the apigenin molecule, thus dispersing the apigenin molecule into the phospholipid molecule at a molecular level.

3.4.3 Fourier transform infrared spectroscopy (FTIR)

The FTIR spectra of pure apigenin, pure Phospholipon[®] 90H, PM, and APLC are shown in Figure 3A, 3B, 3C, and 3D, respectively (all units are cm⁻¹). The spectra of pure apigenin (Figure 3A) revealed characteristic peaks at 3272.34 (O-H), 2894.31 (C-H), 2827.31 (C-H), 1606.77 (C=O), 1622.10 (C=C), 1557.59 (C=C), and 1500.68 (C=C). These observations were in agreement with those reported earlier (Siniša Đorđević et al., 2000). The FTIR spectrum of pure Phospholipon[®] 90H (Figure 3B) revealed the characteristic signals at 2918 and 2850, related to

the C–H stretching present in the long fatty acid chain. Additional signals were also observed at 1738 (C=O stretching in the fatty acid ester), 1236 (P=O stretching), 1091 (P–O–C stretching), and 970 [$-N^+(CH_2)_3$] (Semalty et al., 2012). The spectra of the physical mixture (PM) (Figure 3C) showed peaks that were characteristic of the individual components, i.e. apigenin and Phospholipon[®] 90H at 3304.20, 2917.46, 2849.95, and 1268.25. The spectra of APLC showed broad peaks at 3337.96 (O-H stretching in apigenin), 1237.39 (P=O stretching), and 1092.72 (P–O–C bending). Comparison of the FTIR spectra shows the changes to specific regions of the apigenin molecules due to interaction with phospholipids. Changes to the stretching frequency of the phenolic O-H of apigenin from 3272.34 to 3337.96 in the phytosome suggests that weak intermolecular interactions have been created during the formation of APLC. Moreover, the absorption peaks of phospholipids at 1237.39 and 1092.72 were altered completely. It can thus be inferred that weak intermolecular interactions between apigenin and phospholipid molecules are attributable to the formation of APLC.

3.4.4 Proton nuclear magnetic resonance (¹H-NMR)

Figure 4 (A and B) shows ¹H–NMR spectra of pure apigenin and the prepared APLC, respectively. ¹H chemical shifts are reported in parts per million relative to the TMS peak at δ 0.00. The spectrum of apigenin exhibited characteristic H-shifts described below: ¹H NMR (400 MHz, DMSO-*d*₆): δ 12.93 (s, 1 H, 5-OH), 10.73 (s, 1 H, 4'-OH), 10.28 (s, 1 H, 7-OH), 7.88 (d, J = 8.68 Hz, 2 H, H-2', H-6'), 6.92 (d, J = 8.68 Hz, 2 H, H-3', H-5'), 6.71 (s, 1 H, H-3), 6.44 (d, J = 1.76 Hz, 1 H, H-8), 6.18 (d, J = 1.76 Hz, 1 H, H-6). These chemical shifts were compared with and were found to be consistent with those of pure apigenin established in literature (Li et al., 1997; Semalty et al., 2012) The NMR of Phospholipon[®] 90H (Sharma et al., 2015): ¹H NMR (400 MHz, DMSO-*d*₆) δ 4.85 (1H, s), 4.08-3.96 (1H, m), 3.83-3.62, (2H, m), 3.38 (1H, s), 3.07

(15H, s), 2.95 (8H, d, $J = 6.8$ Hz), 2.27, (1H, s), 1.91 (2H, m), 1.26 (2H, s), 0.95 (23H, s), 0.57 (3H, s). The ^1H NMR of APLC is as follows: δ 12.92 (s, 1 H, 5-OH), 10.70 (s, 1 H, 4'-OH), 10.39 (s, 1 H, 7-OH), 8.225 (2H), 7.88 (d, $J = 8.68$ Hz, 2 H, H-2', H-6'), 7.86, 6.93 (d, $J = 8.68$ Hz, 2 H, H-3', H-5'), 6.71 (s, 1 H, H-3), 6.44 (d, $J = 1.76$ Hz, 1 H, H-8), 6.18 (d, $J = 1.76$ Hz, 1 H, H-6), 3.17 (s, 3H), 1.23 (s, 3H). Upon comparison of the chemical shifts of apigenin alongside APLC, the key differences emerge in the downfield aromatic region ($\delta > 7$) and the upfield aromatic region ($\delta < 4$). The alkyl side chain of the APLC is seen at δ 1.23 and the N-methyl groups correspond to the chemical shift at δ 3.17 (Sikarwar et al., 2008). The formation of molecular aggregates with apigenin is clearly seen by the change in proton signals in the aromatic region. The charged head of the phospholipid molecule is involved in weak intermolecular interactions such as hydrogen bond and ion-dipole interactions with the phenolic (4'-OH and 5-OH) regions of apigenin. This is supported by the lowered intensity of these proton signals and their distinct downfield chemical shifts. This indicates the embedding of apigenin in the phospholipid and thus confirms the formation of the APLC.

3.4.5 Powder x-ray diffractometry (PXRD)

The x-ray diffractograms of pure apigenin, pure Phospholipon[®] 90H, PM, and APLC are shown in Figure 5 (A, B, C, and D, respectively). The diffraction patterns of pure apigenin (Figure 5A) displayed intense and sharp crystalline peaks at $2\theta = 11^\circ, 14^\circ, 16^\circ, 24^\circ, 25^\circ,$ and 26° , characteristic of the crystalline nature of apigenin. Phospholipon[®] 90H (Figure 5B) exhibited a single, relatively broad peak around $2\theta = 20.1^\circ$. The absence of any additional well-defined, sharp, crystalline peaks in the Phospholipon[®] 90H diffractogram indicated the amorphous nature of the phospholipid molecule. These observations are consistent with previously published reports (Cai et al., 2012). The diffractogram of physical mixture (Figure 5C) exhibited few crystalline peaks (related to apigenin) with lower intensity, and a broader peak (associated with

Phospholipon[®] 90H). The decrease in the intensity of crystalline could be due to the lower amount of apigenin in the mixture, interference by the phospholipid molecule, or *in situ* formation of a partial aggregates between apigenin and phospholipid, indicating a partial loss of the crystalline nature of apigenin (Cai et al., 2012). Finally, the diffractogram of APLC exhibited a single broad peak at $2\theta = 20.8^\circ$, and this diffractogram was similar to that of Phospholipon[®] 90H, suggesting that apigenin in APLC may be molecularly dispersed in phospholipid matrix, and may be present in an amorphous form (Yue et al., 2008).

3.4.6 Solubility analysis

The results of the measured solubilities of the pure apigenin, PM, and APLC in water and n-octanol are shown in the Table 4. Pure apigenin was observed to have poor aqueous solubility ($\sim 0.6 \mu\text{g/mL}$), and a relatively higher solubility in n-octanol ($\sim 600 \mu\text{g/mL}$), indicating a rather lipophilic nature. The physical mixture (PM) revealed a modest, but significant increase in the n-octanol solubility ($\sim 635 \mu\text{g/mL}$), and a substantial increase (~ 10 -fold) in the aqueous solubility compared to that of pure apigenin ($p < 0.01$). The prepared phytosome (APLC) however, showed a dramatic, and a highly significant (over 35-fold) increase in the aqueous solubility compared to that of pure apigenin ($p < 0.001$). Partial amorphization (reduced molecular crystallinity) of the apigenin, and the overall amphiphilic nature of the prepared phytosome can be attributed as the main reasons for this observed increase in aqueous solubility (Singh et al., 2012; Xia et al., 2013).

3.5 Functional characterization

3.5.1 *In vitro* dissolution studies

Figure 6 compares the dissolution behavior of pure apigenin with that of the prepared APLC in phosphate buffer (pH 7.0). The release profiles of apigenin and APLC were found to be similar

for the first 5 h. After this point, apigenin dissolution appeared to reach a plateau reaching a maximum of 27.86 % in 8 h. In contrast, the release of apigenin from the APLC continued to increase reaching 50.98% after 12 h. The difference in release rate of apigenin from the two formulations can be attributed to the increased solubility and increased wettability of apigenin in the prepared phytosome (Perrut et al., 2005). Accordingly, (a) pure apigenin has low aqueous solubility which is shown to be improved by the amphiphilic nature of Phospholipon[®] 90H; (b) apigenin is assumed to change from a crystalline state to a partially amorphous state in the APLC, which may extend the rate and extent of dissolution to 12 h; and (c) a change in the structural morphology of crystalline apigenin and the amphiphilic nature of Phospholipon[®] 90H allows for greater wetting of APLC and improved dispersion. Moreover, the sustained release of apigenin from APLC may be assumed to occur via a two-step diffusion process. First, in the presence of aqueous media, apigenin molecules dissociates from the phytosome. Second, the dissociated free apigenin molecules diffuses out of the phospholipid matrix (Dash et al., 2010). Thus, APLC was found to significantly enhance both the rate and the extent of apigenin release compared to pure apigenin.

3.5.2 *In vivo* antioxidant activity

3.5.2.1 *Liver function test*

Carbon tetrachloride (CCl₄) is a well-known hepatotoxin used in animal models. Carbon tetrachloride is reported to be metabolized by hepatic CYP450 enzymes into reactive oxidative species which affect vital organs such as the heart, kidney, brain, blood, and liver (Khan et al., 2012). Free radicals generated from the xenobiotic transformation of carbon tetrachloride (CCl₄) bind covalently to cellular macromolecules (e.g. lipids, nucleic acids, proteins) resulting in oxidative damage. The results of the influence of apigenin and APLC on the hepatic markers of CCl₄-induced rat liver damage are described in Table 5. A significant increase in the marker

enzymes *viz.*, SGOT, SGPT, SALP, and total bilirubin was observed in livers of rats treated with CCl₄ alone. The administration of apigenin (25 mg/kg, p.o.) for 7 consecutive days prevented significantly ($p < 0.05$) this increase in all marker enzymes except SGPT. The administration of APLC (~25 mg/kg apigenin) also prevented the CCl₄-induced increase in the levels of all liver marker enzymes (including SGPT), and with higher significance ($p < 0.01$). The results thus demonstrate improved hepatoprotective activity of APLC compared to that observed with pure apigenin.

3.5.2.2 In vivo antioxidant marker enzyme estimation

Levels of liver enzymes such as glutathione (GSH), superoxide dismutase (SOD), catalase (CAT), and lipid peroxidase (LPO) have been reported as reliable indicators of antioxidant activity (Khan et al., 2012; Maiti et al., 2005; Recknagel et al., 1989). Apigenin has been documented as having excellent antioxidant and hepatoprotective properties (Romanova et al., 2001). In the current study, we examine the effects of pure apigenin and APLC on the levels of GSH, SOD, CAT, and LPO on CCl₄-treated and naïve mice (Figure 7). CCl₄-treated animals showed significantly reduced ($p < 0.01$) levels of GSH compared to the control group of normal animals. The group treated with pure apigenin (25 mg/kg, p.o.) significantly ($p < 0.05$) prevented the CCl₄-induced reduction in GSH levels. The animal group treated with APLC (~25 mg/kg apigenin, p.o.) also showed a prevention of CCl₄-induced lowering of GSH levels, albeit with a higher significance ($p < 0.01$) in the liver homogenate. The levels of SOD were found to be significantly ($p < 0.01$) reduced as a result of CCl₄ treatment. Treatment with pure apigenin (25 mg/kg, p.o.) failed to significantly prevent CCl₄-induced reduction in SOD levels. In comparison, the APLC (~25 mg/kg apigenin, p.o.) treatment was found to result in a significant ($p < 0.01$) prevention of CCl₄-induced lowering of SOD levels. CAT levels were found to

significantly ($p < 0.01$) decrease as a result of CCl_4 treatment. CCl_4 -treated animals showed significantly reduced (** $p < 0.01$) CAT level as compared to normal animals. The group treated with pure apigenin (25 mg/kg, p.o.) significantly ($p < 0.05$) prevented this CCl_4 -induced reduction in CAT levels. The animal group treated with APLC (~25 mg/kg apigenin, p.o.) also showed a prevention of CCl_4 -induced lowering of CAT levels, albeit with a higher significance ($p < 0.01$). CCl_4 treatment was found to result in significantly ($p < 0.01$) increased LPO levels when compared to normal rats. The group treated with pure apigenin (25 mg/kg, p.o.) significantly ($p < 0.05$) prevented this CCl_4 -induced increase in LPO levels. The animal group treated with APLC (~25 mg/kg apigenin, p.o.) also showed a prevention of CCl_4 -induced increase of LPO levels, albeit with a higher significance ($p < 0.01$).

3.5.2.3 Histopathological studies

A visual assessment of the influence of pure apigenin or APLC treatment on the CCl_4 -induced liver damage was provided by the histopathological investigation of rat liver tissues. Figure 8 (A, B, C, and D) shows hematoxylin-eosin stained microscopic (400 \times) images of liver tissues for the treatment groups, i.e. Tween[®] 20, CCl_4 -treated, pure apigenin + CCl_4 , or APLC+ CCl_4 , respectively. As shown in Figure 8A, the treatment group that received Tween[®] 20 (1%, v/v) exhibited well-preserved cellular organelles indicating healthy, well-functioning liver tissue and hepatic cells. The animals treated with CCl_4 alone (Figure 8B) showed visible damage and degeneration of parenchymal cells, degeneration of the fatty tissues (steatosis), and a significant damage to the central lobular region. The administration of pure apigenin (25 mg/kg, p.o.) demonstrated a hepatoprotective activity against the CCl_4 -induced hepatic toxicity (Figure 8C). Similarly, the treatment group that received APLC (~25 mg/kg apigenin, p.o.) showed a significant protection against CCl_4 -induced liver damages (Figure 8D). Both pure apigenin and

APLC treatments appear to restore the normal anatomy of the hepatic cellular structures, which can be attributed to the antioxidant properties of apigenin.

3.5.3 Oral bioavailability studies

The chromatographic conditions were optimized to improve peak resolution, signal-to-noise ratio, and the duration of sample analysis. Apigenin and quercetin (internal standard) are polar molecules and different buffers were tested to obtain a mobile phase that produced optimal sensitivity and efficiency. Methanol was used as mobile phase and the samples analyzed by LC-MS/MS with an acceptable run of 5.0 min. We observed that adding formic acid (0.1% v/v) to the mobile phase greatly improved the electrospray ionization efficiency of the analytes in the positive ion mode. An initial UV scan revealed two peaks for apigenin (268 nm and 335 nm), and a single peak for quercetin (368 nm). The choice of an appropriate detection wavelength (λ) is critical to ensure a reliable detection of all components of the analyte. Consequently, 350 nm was selected as the wavelength of detection for current analysis.

Apigenin was initially characterized according to its mass spectra from a syringe pump infusion analysis, and the daughter ions were revealed in SRM. The heated-electrospray ionization (H-ESI) was employed for improved sensitivity and fragmentation. We observed that the optimum de-clustering potential for apigenin was +4500V, and thus positive ion mode was found to be more sensitive for the analysis of apigenin. We also found that it was ideal to use the SRM mode was ideal. In this mode only the daughter ions of apigenin and quercetin were fragmented at a collision energy of 39V using nitrogen as a collision medium. In the full-scan mass spectra, the daughter ions were observed to be stable and exhibited a high abundance. The daughter ions were thus selected as precursor ions for MS/MS fragmentation analysis of apigenin

and quercetin. The optimized mass transition ion-pairs (m/z) for quantification of apigenin and quercetin were established at 271.2/119.0 and 303.0/152.9, respectively.

The liquid-liquid extraction, protein precipitation, and solid-liquid extraction are among the commonly used techniques for extraction of drugs from a plasma matrix. Solid-liquid extraction demonstrates excellent recovery and reproducibility. However this technique is complicated and expensive. This limits its applications for a rapid processing of multiple samples for bioequivalence and pharmacokinetics studies (Yang et al., 2013). The protein precipitation technique exhibits low sample recovery and higher costs due to the use of multiple extracting solvents (Barve et al., 2009; DuPont et al., 2004). In the current study, liquid-liquid extraction using hydrochloric acid (0.2M) was used to process the plasma samples. During the experimental trials, we found that the apigenin and quercetin were easily detected after hydrolysis of the plasma with high recovery and accuracy (Chen et al., 2010; Chen et al., 2012; Duan et al., 2011). The LC-MS/MS technique was thus effectively applied to monitor the concentrations of apigenin in rat plasma for pharmacokinetic evaluation.

The mean plasma concentration-time profiles of apigenin in the plasma of animals treated with pure apigenin (100 mg/kg, p.o.) or APLC (~100 mg/kg apigenin, p.o.) are shown in Figure 9. The results show a significant increase in the plasma concentration of apigenin in groups treated with APLC up to 10 h. The plasma concentration-time profiles of both treatment groups, i.e. pure apigenin and APLC showed a bimodal pattern. These results are in agreement with previous reports where, this bimodal profiles are thought to occur due to enterohepatic recirculation (Wan et al., 2007; Zhang et al., 2009). The key pharmacokinetic parameters, as estimated using a statistical software (WinNonlin[®], Version 4.1, Certara USA Inc., Princeton, NJ, USA) are listed in Table 6. The analysis of data revealed that all pharmacokinetic parameters

indicative of relative bioavailability, i.e. C_{max} , T_{max} , and $AUC_{0-\infty}$ were significantly higher in animals treated with APLC compared to those treated with pure apigenin. The values of elimination half-life ($t_{1/2el}$) and the elimination rate constant (K_{el}) remained unchanged for both treatment groups. The clearance (cl/F) and volume of distribution (V_z/F) of apigenin was found to be significantly lower in the group treated with APLC. These observations indicated a longer residence and resulting prolonged duration of action of apigenin after APLC administration. The computed bioavailability (F) of apigenin after APLC administration was found to be 82.02%.

The observed enhancement of the relative bioavailability of apigenin after single oral administration of APLC can be attributed to two main factors: (1) phospholipid-based formation of molecular aggregates which improves the aqueous solubility of apigenin, leading to enhanced intestinal absorption, and, (2) the role of amphiphilic phospholipids as a vesicular carrier matrix for apigenin, which may protect it from hepatic first-pass metabolism. While we have observed an improved *in vivo* bioavailability of apigenin with the prepared APLC, it is important to note that several factors e.g. dietary lipid intake, can significantly influence the rate and extent of absorption and the overall bioavailability of drugs via these systems. As pointed out by Fong et al., the evaluation of solubility and permeability, and the use of appropriate biorelevant media for such evaluation is critical in understanding the biopharmaceutical behavior of lipid-based formulations (Fong et al., 2016).

4 Conclusions

The present work reveals the excellent potential of phospholipid-base molecular aggregates for improving the solubility, oral bioavailability and *in vivo* antioxidant activity of apigenin, a BCS Class II drug. The APLC was formulated with the help of a solvent evaporation method and optimized using a full factorial design (3^2) strategy. The APLC formation was supported by

DSC, FTIR, ¹H-NMR, and PXRD analysis. The data clearly pointed towards the presence of non-covalent bonding interactions, viz, hydrogen bonding, ion-dipole and van der Waals interactions, as key factors in the formation of a stable APLC. Solubility studies demonstrated increased solubility of APLC in water as compared to PM or pure apigenin. Furthermore, the rate and extent of *in vitro* apigenin release was significantly enhanced when compared to the suspension of pure apigenin. In a CCl₄-induced hepatotoxicity model in rats, APLC restored the antioxidant enzymes to a significant level, relative to free apigenin. APLC also enhanced oral bioavailability of apigenin by demonstrating increased C_{max} , T_{max} , and AUC parameters as compared to apigenin. This study validates the value of employing phospholipids in preparing phytosomes with phytoconstituents of low solubility to improve their solubility, oral bioavailability, and pharmacological properties.

5 Acknowledgement

The authors are thankful to R.T.M. Nagpur University, Nagpur, Maharashtra, India, for the financial assistance to support this research project (DS/RTM/2013–14/2076).

6 References

- Shukla, S., Gupta, S., 2010. Apigenin: A Promising Molecule for Cancer Prevention. *Pharm. Res.* 27, 962-978.
- Peterson, J., Dwyer, J., 1998. Flavonoids: Dietary occurrence and biochemical activity. *Nutr. Res.* 18, 1995-2018.
- Prince Vijeya Singh, J., Selvendiran, K., Mumtaz Banu, S., Padmavathi, R., Sakthisekaran, D., 2004. Protective role of Apigenin on the status of lipid peroxidation and antioxidant defense against hepatocarcinogenesis in Wistar albino rats. *Phytomedicine* 11, 309-314.
- Stanojević, L., Stanković, M., Nikolić, V., Nikolić, L., Ristić, D., Čanadanovic-Brunet, J., Tumbas, V., 2009. Antioxidant Activity and Total Phenolic and Flavonoid Contents of *Hieracium pilosella* L. Extracts. *Sensors* 9, 5702-5714.
- Taleb-Contini, S.H., Salvador, M.J., Watanabe, E., Ito, I.Y., Oliveira, D.C.R.d., 2003. Antimicrobial activity of flavonoids and steroids isolated from two *Chromolaena* species. *Rev. Bras. Cienc. Farm.* 39, 403-408.
- Funakoshi-Tago, M., Nakamura, K., Tago, K., Mashino, T., Kasahara, T., 2011. Anti-inflammatory activity of structurally related flavonoids, Apigenin, Luteolin and Fisetin. *Int. Immunopharmacol.* 11, 1150-1159.

Rithidech, K.N., Tungjai, M., Reungpatthanaphong, P., Honikel, L., Simon, S.R., 2012. Attenuation of oxidative damage and inflammatory responses by apigenin given to mice after irradiation. *Mutation Research/Genetic Toxicology and Environmental Mutagenesis* 749, 29-38.

Johnson, J.L., Gonzalez de Mejia, E., 2013. Interactions between dietary flavonoids apigenin or luteolin and chemotherapeutic drugs to potentiate anti-proliferative effect on human pancreatic cancer cells, in vitro. *Food Chem. Toxicol.* 60, 83-91.

Shibata, C., Ohno, M., Otsuka, M., Kishikawa, T., Goto, K., Muroyama, R., Kato, N., Yoshikawa, T., Takata, A., Koike, K., 2014. The flavonoid apigenin inhibits hepatitis C virus replication by decreasing mature microRNA122 levels. *Virology* 462-463, 42-48.

Choi, J.S., Nurul Islam, M., Yousof Ali, M., Kim, E.J., Kim, Y.M., Jung, H.A., 2014. Effects of C-glycosylation on anti-diabetic, anti-Alzheimer's disease and anti-inflammatory potential of apigenin. *Food Chem. Toxicol.* 64, 27-33.

Choudhury, D., Ganguli, A., Dastidar, D.G., Acharya, B.R., Das, A., Chakrabarti, G., 2013. Apigenin shows synergistic anticancer activity with curcumin by binding at different sites of tubulin. *Biochimie* 95, 1297-1309.

Ruela-de-Sousa, R.R., Fuhler, G.M., Blom, N., Ferreira, C.V., Aoyama, H., Peppelenbosch, M.P., 2010. Cytotoxicity of apigenin on leukemia cell lines: implications for prevention and therapy. *Cell Death Dis.* 1, e19.

Zhang, J., Liu, D., Huang, Y., Gao, Y., Qian, S., 2012. Biopharmaceutics classification and intestinal absorption study of apigenin. *Int. J. Pharm.* 436, 311-317.

Griffiths, L.A., Smith, G.E., 1972. Metabolism of apigenin and related compounds in the rat. Metabolite formation in vivo and by the intestinal microflora in vitro. *Biochem. J.* 128, 901-911.

Chen, Z., Kong, S., Song, F., Li, L., Jiang, H., 2012. Pharmacokinetic study of luteolin, apigenin, chrysoeriol and diosmetin after oral administration of Flos Chrysanthemi extract in rats. *Fitoterapia* 83, 1616-1622.

Arsić, I., Tadić, V., Vlaović, D., Homšek, I., Vesić, S., Isailović, G., Vuleta, G., 2011. Preparation of novel apigenin-enriched, liposomal and non-liposomal, antiinflammatory topical formulations as substitutes for corticosteroid therapy. *Phytother. Res.* 25, 228-233.

Al Shaal, L., Shegokar, R., Müller, R.H., 2011. Production and characterization of antioxidant apigenin nanocrystals as a novel UV skin protective formulation. *Int. J. Pharm.* 420, 133-140.

Zhao, L., Zhang, L., Meng, L., Wang, J., Zhai, G., 2013. Design and evaluation of a self-microemulsifying drug delivery system for apigenin. *Drug Dev. Ind. Pharm.* 39, 662-669.

Munyendo, W.L., Zhang, Z., Abbad, S., Waddad, A.Y., Lv, H., Baraza, L.D., Zhou, J., 2013. Micelles of TPGS modified apigenin phospholipid complex for oral administration: preparation, in vitro and in vivo evaluation. *J. Biomed. Nanotechnol.* 9, 2034-2047.

Karthivashan, G., Masarudin, M.J., Kura, A.U., Abas, F., Fakurazi, S., 2016. Optimization, formulation, and characterization of multiflavonoids-loaded flavanosome by bulk or sequential technique. *Int. J. Nanomedicine* 11, 3417-3434.

Shen, L.N., Zhang, Y.T., Wang, Q., Xu, L., Feng, N.P., 2014. Enhanced in vitro and in vivo skin deposition of apigenin delivered using ethosomes. *Int. J. Pharm.* 460, 280-288.

Pawlikowska-Pawlega, B., Misiak, L.E., Zarzyka, B., Paduch, R., Gawron, A., Gruszecki, W.I., 2013. FTIR, (1)H NMR and EPR spectroscopy studies on the interaction of flavone apigenin with dipalmitoylphosphatidylcholine liposomes. *Biochim. Biophys. Acta* 1828, 518-527.

Semalty, A., Semalty, M., Rawat, B.S., Singh, D., Rawat, M.S., 2009. Pharmacosomes: the lipid-based new drug delivery system. *Expert Opin. Drug Deliv.* 6, 599-612.

Saoji, S.D., Raut, N.A., Dhore, P.W., Borkar, C.D., Popielarczyk, M., Dave, V.S., 2016. Preparation and Evaluation of Phospholipid-Based Complex of Standardized Centella Extract (SCE) for the Enhanced Delivery of Phytoconstituents. *AAPS J.* 18, 102-114.

Ruan, J., Liu, J., Zhu, D., Gong, T., Yang, F., Hao, X., Zhang, Z., 2010. Preparation and evaluation of self-nanoemulsified drug delivery systems (SNEDDSs) of matrine based on drug-phospholipid complex technique. *Int. J. Pharm.* 386, 282-290.

Yue, P.-F., Yuan, H.-L., Li, X.-Y., Yang, M., Zhu, W.-F., 2010. Process optimization, characterization and evaluation in vivo of oxymatrine-phospholipid complex. *Int. J. Pharm.* 387, 139-146.

Zhang, J., Tang, Q., Xu, X., Li, N., 2013. Development and evaluation of a novel phytosome-loaded chitosan microsphere system for curcumin delivery. *Int. J. Pharm.* 448, 168-174.

Semalty, A., Semalty, M., Singh, D., Rawat, M.S.M., 2012. Phyto-phospholipid complex of catechin in value added herbal drug delivery. *J. Inclusion Phenom. Macrocyclic Chem.* 73, 377-386.

Singh, D., Rawat, M.S.M., Semalty, A., Semalty, M., 2012. Chrysophanol-phospholipid complex. *J. Therm. Anal. Calorim.* 111, 2069-2077.

Semalty, A., Tanwar, Y.S., Semalty, M., 2014. Preparation and characterization of cyclodextrin inclusion complex of naringenin and critical comparison with phospholipid complexation for improving solubility and dissolution. *J. Therm. Anal. Calorim.* 115, 2471-2478.

Semalty, A., Semalty, M., Rawat, M.S., Franceschi, F., 2010. Supramolecular phospholipids-polyphenolics interactions: the PHYTOSOME strategy to improve the bioavailability of phytochemicals. *Fitoterapia* 81, 306-314.

Semalty, A., 2014. Cyclodextrin and phospholipid complexation in solubility and dissolution enhancement: a critical and meta-analysis. *Expert Opin. Drug Deliv.* 11, 1255-1272.

Bhattacharyya, S., Majhi, S., Saha, B.P., Mukherjee, P.K., 2014. Chlorogenic acid-phospholipid complex improve protection against UVA induced oxidative stress. *Journal of Photochemistry and Photobiology B: Biology* 130, 293-298.

Maiti, K., Mukherjee, K., Gantait, A., Saha, B.P., Mukherjee, P.K., 2007. Curcumin-phospholipid complex: Preparation, therapeutic evaluation and pharmacokinetic study in rats. *Int. J. Pharm.* 330, 155-163.

Tan, Q., Liu, S., Chen, X., Wu, M., Wang, H., Yin, H., He, D., Xiong, H., Zhang, J., 2012. Design and evaluation of a novel evodiamine-phospholipid complex for improved oral bioavailability. *AAPS PharmSciTech* 13, 534-547.

Maiti, K., Mukherjee, K., Murugan, V., Saha, B.P., Mukherjee, P.K., 2009. Exploring the Effect of Hesperetin-HSPC Complex—A Novel Drug Delivery System on the In Vitro Release, Therapeutic Efficacy and Pharmacokinetics. *AAPS PharmSciTech* 10, 943.

Reitman, S., Frankel, S., 1957. A colorimetric method for the determination of serum glutamic oxalacetic and glutamic pyruvic transaminases. *Am. J. Clin. Pathol.* 28, 56-63.

Kind, P.R.N., King, E.J., 1954. Estimation of Plasma Phosphatase by Determination of Hydrolysed Phenol with Amino-antipyrine. *J. Clin. Pathol.* 7, 322-326.

Malloy, H.T., Evelyn, K.A., 1937. The Determination of Bilirubin with the Photoelectric Colorimeter. *J. Biol. Chem.* 119, 481-490.

Ellman, G.L., 1959. Tissue sulfhydryl groups. *Arch. Biochem. Biophys.* 82, 70-77.

Marklund, S., Marklund, G., 1974. Involvement of the superoxide anion radical in the autoxidation of pyrogallol and a convenient assay for superoxide dismutase. *Eur. J. Biochem.* 47, 469-474.

Stocks, J., Dormandy, T.L., 1971. The Autoxidation of Human Red Cell Lipids Induced by Hydrogen Peroxide. *Br. J. Haematol.* 20, 95-111.

Beers, R.F., Jr., Sizer, I.W., 1952. A spectrophotometric method for measuring the breakdown of hydrogen peroxide by catalase. *J. Biol. Chem.* 195, 133-140.

Duan, K., Yuan, Z., Guo, W., Meng, Y., Cui, Y., Kong, D., Zhang, L., Wang, N., 2011. LC-MS/MS determination and pharmacokinetic study of five flavone components after solvent extraction/acid hydrolysis in rat plasma after oral administration of *Verbena officinalis* L. extract. *J. Ethnopharmacol.* 135, 201-208.

Chen, T., Li, L.P., Lu, X.Y., Jiang, H.D., Zeng, S., 2007. Absorption and excretion of luteolin and apigenin in rats after oral administration of *Chrysanthemum morifolium* extract. *J. Agric. Food Chem.* 55, 273-277.

Jabbari, M., Gharib, F., 2012. Solvent dependence on antioxidant activity of some water-insoluble flavonoids and their cerium(IV) complexes. *J. Mol. Liq.* 168, 36-41.

Agency for Toxic Substances & Disease Registry, C., 2012, Toxicological Profile for 1,4 Dioxane, Control, C.f.D., Atlanta Georgia, Center for Disease Control, <https://www.atsdr.cdc.gov/toxprofiles/tp.asp?id=955&tid=199>, 12/04/2016

Qin, X., Yang, Y., Fan, T.T., Gong, T., Zhang, X.N., Huang, Y., 2010. Preparation, characterization and in vivo evaluation of bergenin-phospholipid complex. *Acta Pharmacol. Sin.* 31, 127-136.

LeFevre, M.E., Olivo, R., Vanderhoff, J.W., Joel, D.D., 1978. Accumulation of latex in Peyer's patches and its subsequent appearance in villi and mesenteric lymph nodes. *Proc. Soc. Exp. Biol. Med.* 159, 298-302.

Savic, R., Luo, L., Eisenberg, A., Maysinger, D., 2003. Micellar nanocontainers distribute to defined cytoplasmic organelles. *Science* 300, 615-618.

Dhore, P.W., Dave, V.S., Saoji, S.D., Bobde, Y.S., Mack, C., Raut, N.A., 2016. Enhancement of the aqueous solubility and permeability of a poorly water soluble drug ritonavir via lyophilized milk-based solid dispersions. *Pharm. Dev. Technol.*, 1-13.

Freitas, C., Müller, R.H., 1998. Effect of light and temperature on zeta potential and physical stability in solid lipid nanoparticle (SLN™) dispersions. *Int. J. Pharm.* 168, 221-229.

Li, J., Liu, P., Liu, J.-P., Yang, J.-K., Zhang, W.-L., Fan, Y.-Q., Kan, S.-L., Cui, Y., Zhang, W.-J., 2013. Bioavailability and foam cells permeability enhancement of Salvianolic acid B pellets based on drug-phospholipids complex technique. *Eur. J. Pharm. Biopharm.* 83, 76-86.

Yanyu, X., Yunmei, S., Zhipeng, C., Qineng, P., 2006. The preparation of silybin-phospholipid complex and the study on its pharmacokinetics in rats. *Int. J. Pharm.* 307, 77-82.

Galasso, V., Asaro, F., Berti, F., Pergolese, B., Kovač, B., Pichierri, F., 2006. On the molecular and electronic structure of matrine-type alkaloids. *Chem. Phys.* 330, 457-468.

Lasonder, E., Weringa, W.D., 1990. An NMR and DSC study of the interaction of phospholipid vesicles with some anti-inflammatory agents. *J. Colloid Interface Sci.* 139, 469-478.

Venema, F.R., Weringa, W.D., 1988. The interactions of phospholipid vesicles with some anti-inflammatory agents. *J. Colloid Interface Sci.* 125, 484-492.

Siniša Đorđević, Milorad Cakić, Amr, S., 2000. The Extraction of Apigenin and Luteolin From the Sage *Salvia Officinalis* L. From Jordan. *Facta Universitatis* 1, 86-93.

Li, B., Robinson, D.H., Birt, D.F., 1997. Evaluation of properties of apigenin and [G-3H]apigenin and analytic method development. *J. Pharm. Sci.* 86, 721-725.

Sharma, S., Roy, R.K., Shrivastava, B., 2015. Antiproliferative effect of Phytosome complex of Methanolic extract of *Terminalia Arjuna* bark on Human Breast Cancer Cell Lines (MCF-7) *International Journal of Drug Development and Research* 7, 173-182.

Sikarwar, M.S., Sharma, S., Jain, A.K., Parial, S.D., 2008. Preparation, Characterization and Evaluation of Marsupsin–Phospholipid Complex. *AAPS PharmSciTech* 9, 129-137.

Cai, X., Luan, Y., Jiang, Y., Song, A., Shao, W., Li, Z., Zhao, Z., 2012. Huperzine A–phospholipid complex-loaded biodegradable thermosensitive polymer gel for controlled drug release. *Int. J. Pharm.* 433, 102-111.

Yue, P.F., Zhang, W.J., Yuan, H.L., Yang, M., Zhu, W.F., Cai, P.L., Xiao, X.H., 2008. Process optimization, characterization and pharmacokinetic evaluation in rats of ursodeoxycholic acid–phospholipid complex. *AAPS PharmSciTech* 9, 322-329.

Xia, H.J., Zhang, Z.H., Jin, X., Hu, Q., Chen, X.Y., Jia, X.B., 2013. A novel drug-phospholipid complex enriched with micelles: preparation and evaluation in vitro and in vivo. *Int. J. Nanomedicine* 8, 545-554.

Perrut, M., Jung, J., Leboeuf, F., 2005. Enhancement of dissolution rate of poorly-soluble active ingredients by supercritical fluid processes: Part I: Micronization of neat particles. *Int. J. Pharm.* 288, 3-10.

Dash, S., Murthy, P.N., Nath, L., Chowdhury, P., 2010. Kinetic modeling on drug release from controlled drug delivery systems. *Acta Pol. Pharm.* 67, 217-223.

Khan, R.A., Khan, M.R., Sahreen, S., Shah, N.A., 2012. Hepatoprotective activity of *Sonchus asper* against carbon tetrachloride-induced injuries in male rats: a randomized controlled trial. *BMC Complement. Altern. Med.* 12, 1-8.

Maiti, K., Mjukherjee, K., Gantait, A., Ahmed, H.N., Saha, B.P., Mukherjee, P.K., 2005. Enhanced Therapeutic Benefit of Quercetin–Phospholipid Complex in Carbon Tetrachloride–Induced Acute Liver Injury in Rats: A Comparative Study. *Iranian Journal of Pharmacology & Therapeutics* 4, 84-90.

Recknagel, R.O., Glende, E.A., Dolak, J.A., Waller, R.L., 1989. Mechanisms of carbon tetrachloride toxicity. *Pharmacol. Ther.* 43, 139-154.

Romanova, D., Vachalkova, A., Cipak, L., Ovesna, Z., Rauko, P., 2001. Study of antioxidant effect of apigenin, luteolin and quercetin by DNA protective method. *Neoplasma* 48, 104-107.

Yang, J., Lv, F., Chen, X.-q., Cui, W.-x., Chen, L.-h., Wen, X.-d., Wang, Q., 2013. Pharmacokinetic study of major bioactive components in rats after oral administration of extract of *Ilex hainanensis* by high-performance liquid chromatography/electrospray ionization mass spectrometry. *J. Pharm. Biomed. Anal.* 77, 21-28.

Barve, A., Chen, C., Hebbar, V., Desiderio, J., Saw, C.L., Kong, A.N., 2009. Metabolism, oral bioavailability and pharmacokinetics of chemopreventive kaempferol in rats. *Biopharm. Drug Dispos.* 30, 356-365.

DuPont, M.S., Day, A.J., Bennett, R.N., Mellon, F.A., Kroon, P.A., 2004. Absorption of kaempferol from endive, a source of kaempferol-3-glucuronide, in humans. *Eur. J. Clin. Nutr.* 58, 947-954.

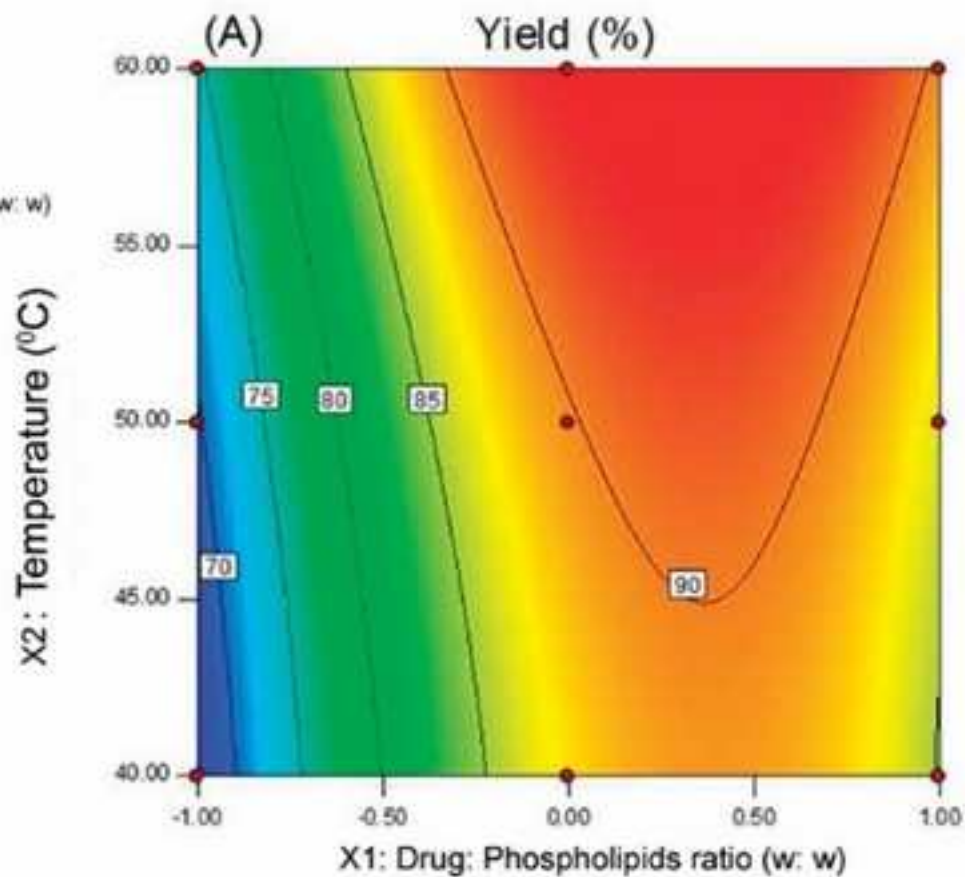
Chen, Z.-p., Sun, J., Chen, H.-x., Xiao, Y.-y., Liu, D., Chen, J., Cai, H., Cai, B.-c., 2010. Comparative pharmacokinetics and bioavailability studies of quercetin, kaempferol and isorhamnetin after oral administration of *Ginkgo biloba* extracts, *Ginkgo biloba* extract phospholipid complexes and *Ginkgo biloba* extract solid dispersions in rats. *Fitoterapia* 81, 1045-1052.

Wan, L., Guo, C., Yu, Q., Li, Y., Wang, X., Wang, X., Chen, C., 2007. Quantitative determination of apigenin and its metabolism in rat plasma after intravenous bolus administration by HPLC coupled with tandem mass spectrometry. *J. Chromatogr. B* 855, 286-289.

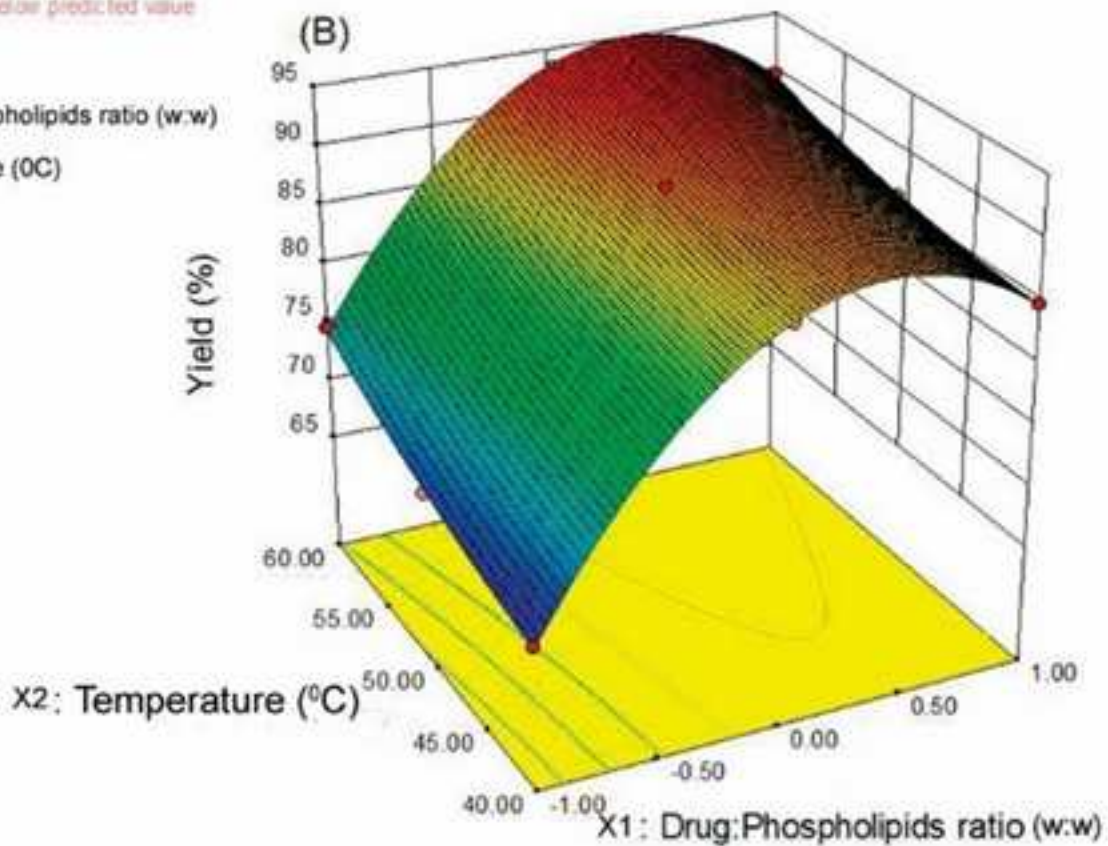
Zhang, Q., Zhang, Y., Zhang, Z., Lu, Z., 2009. Sensitive determination of kaempferol in rat plasma by high-performance liquid chromatography with chemiluminescence detection and application to a pharmacokinetic study. *J. Chromatogr. B* 877, 3595-3600.

Fong, S.Y., Martins, S.M., Brandl, M., Bauer-Brandl, A., 2016. Solid Phospholipid Dispersions for Oral Delivery of Poorly Soluble Drugs: Investigation Into Celecoxib Incorporation and Solubility-In Vitro Permeability Enhancement. *J. Pharm. Sci.* 105, 1113-1123.

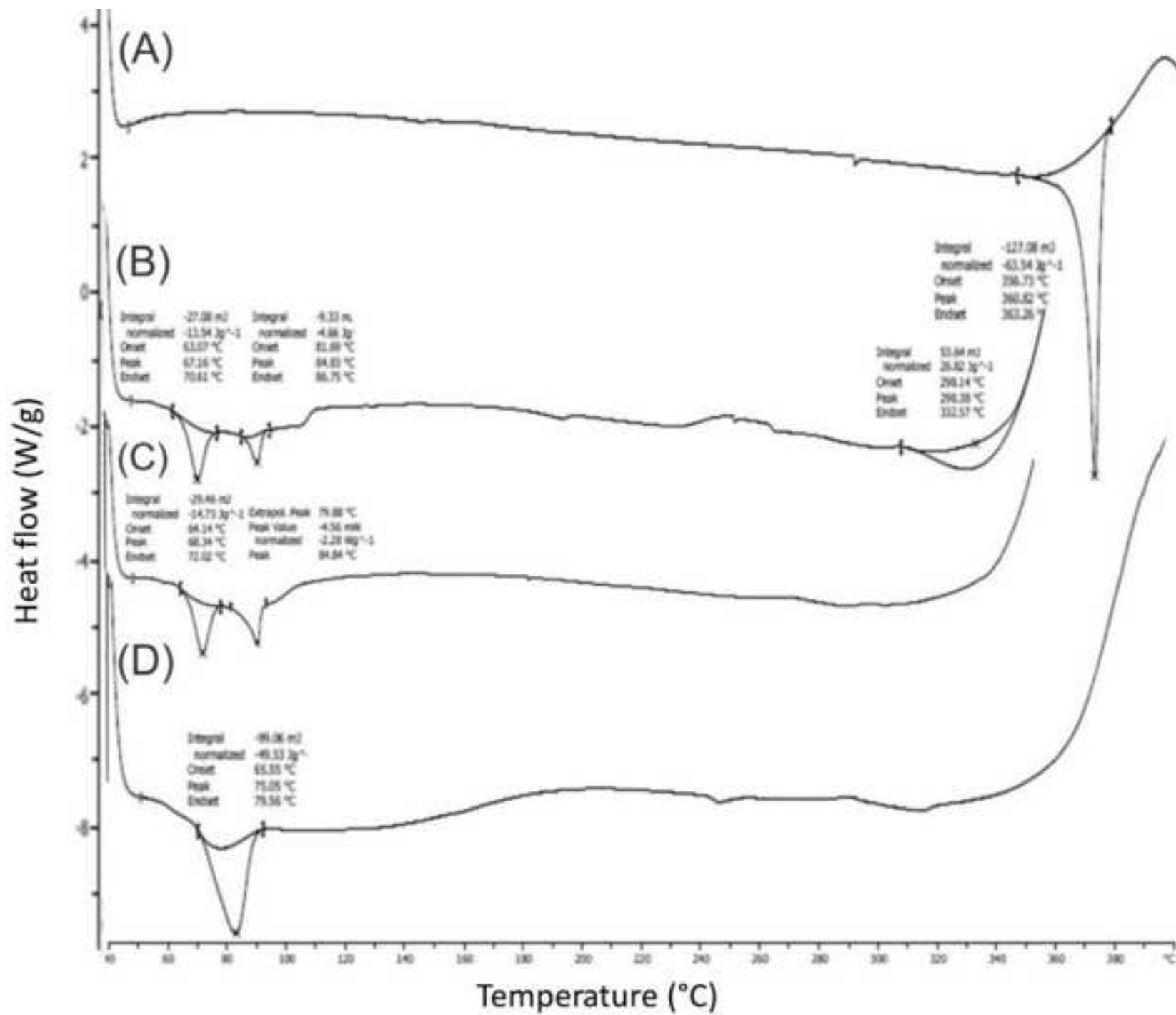
Design-Expert® Software
 Factor Coding: Actual
 Yield (%)
 ● Design points
 93.36
 66.84
 X1: Drug: Phospholipids ratio (w:w)
 X2: Temperature (°C)



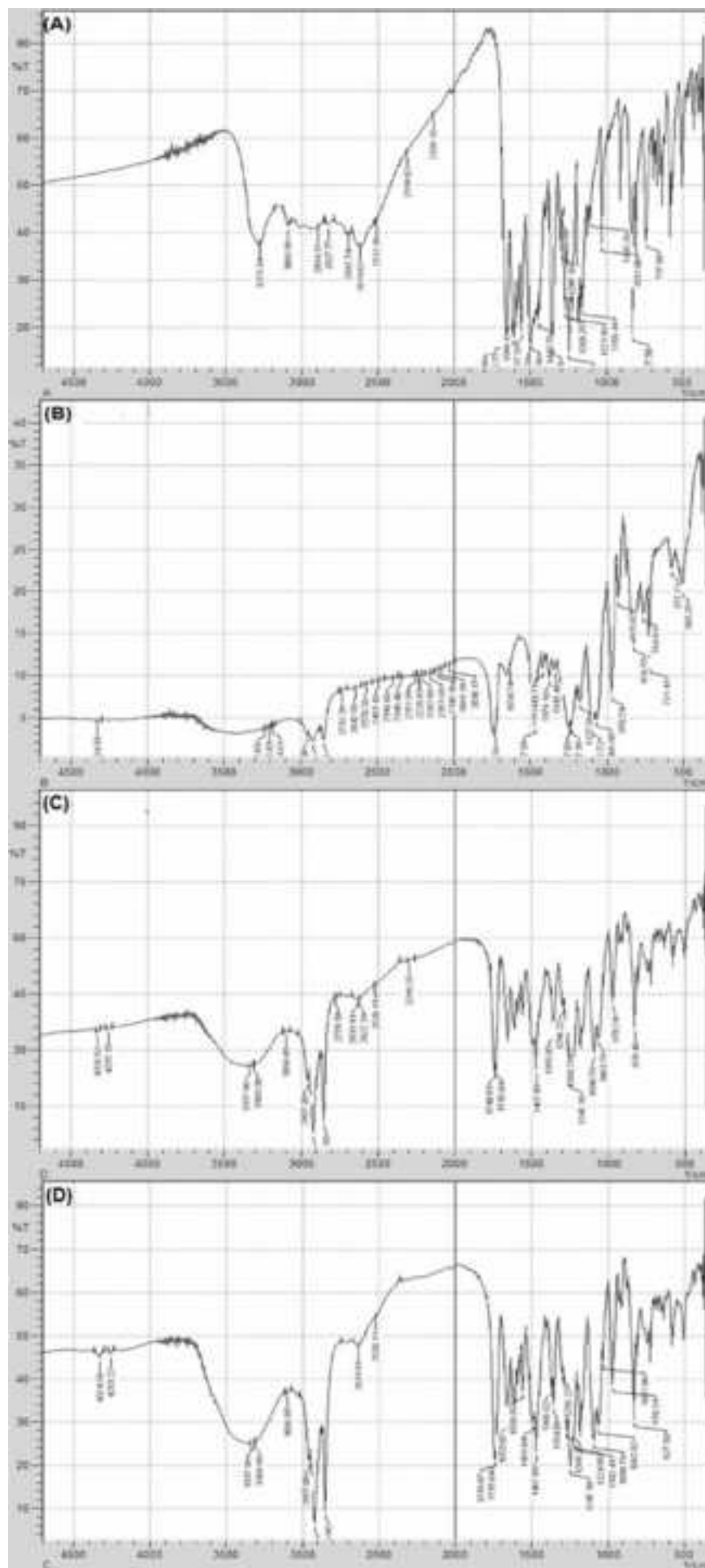
Design-Expert® Software
 Factor Coding: Actual
 Yield (%)
 ● Design points above predicted value
 ● Design points below predicted value
 93.36
 66.84
 X1: Drug: Phospholipids ratio (w:w)
 X2: Temperature (°C)



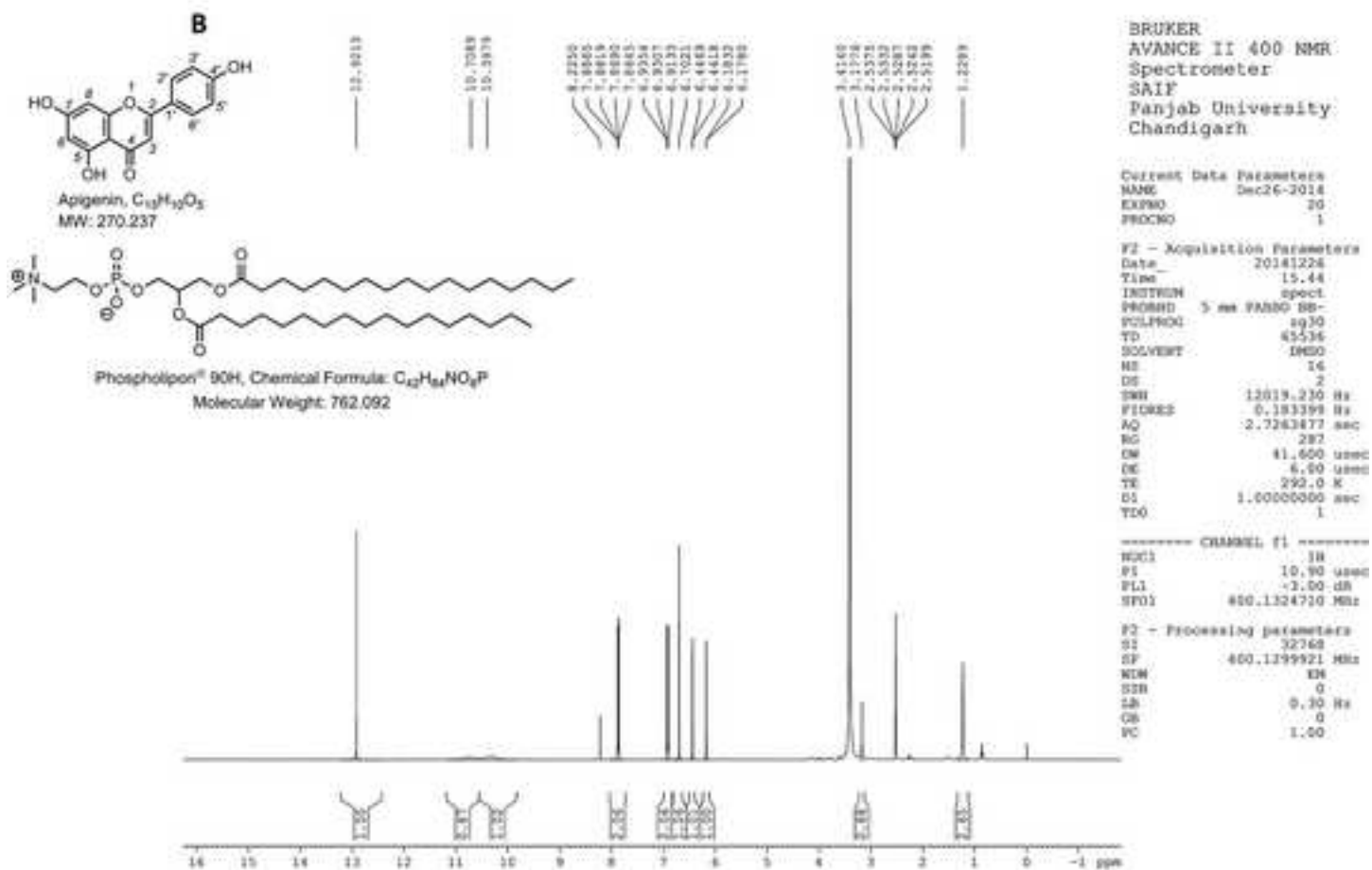
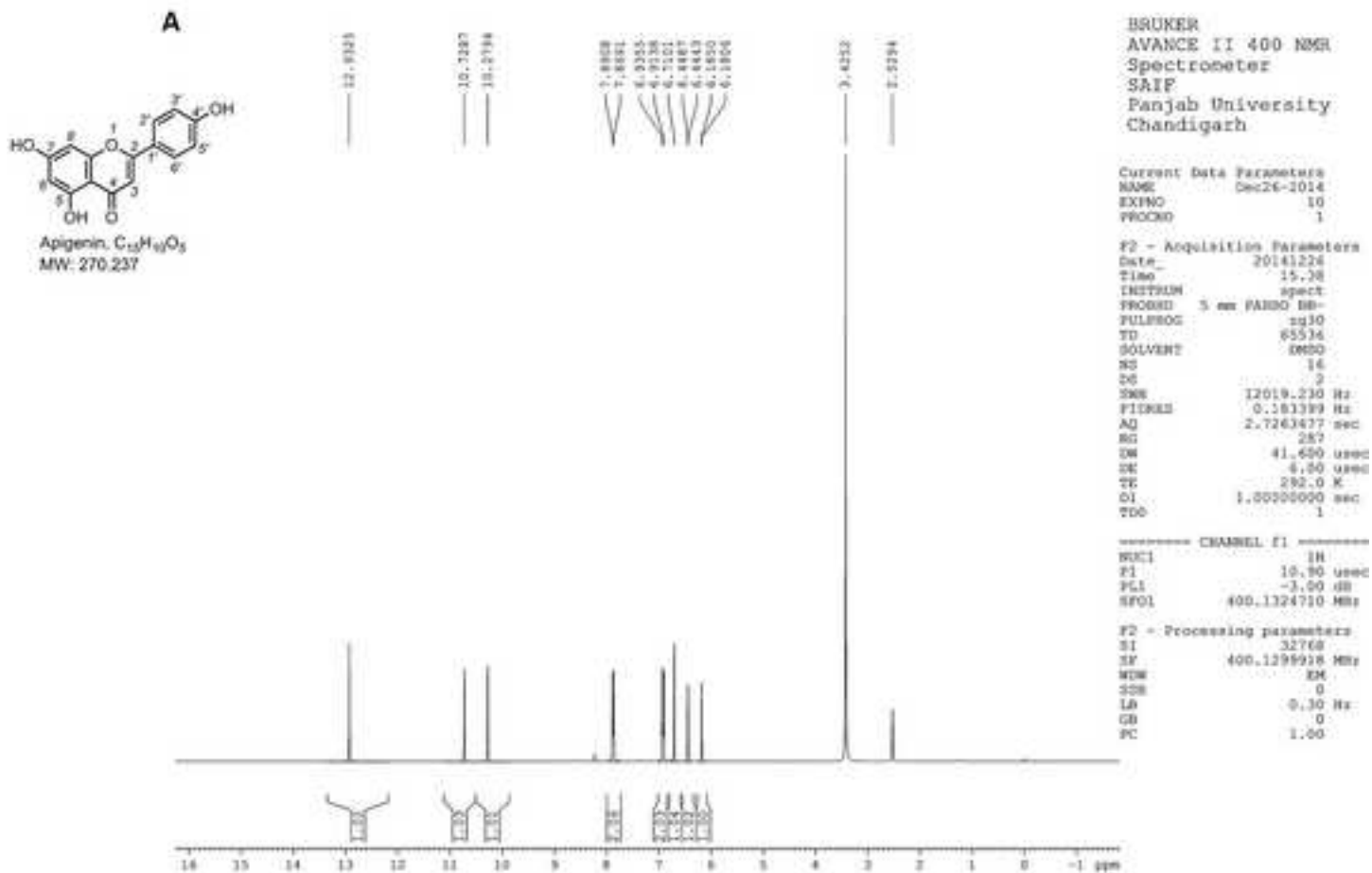
Figure(s)



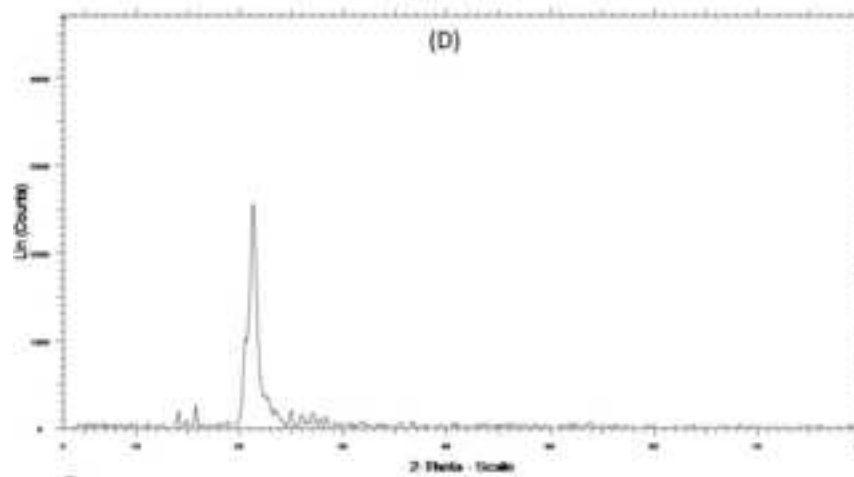
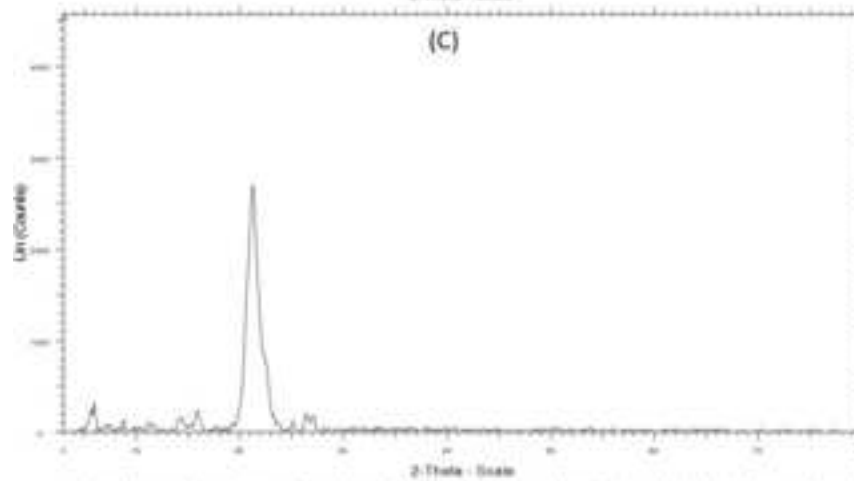
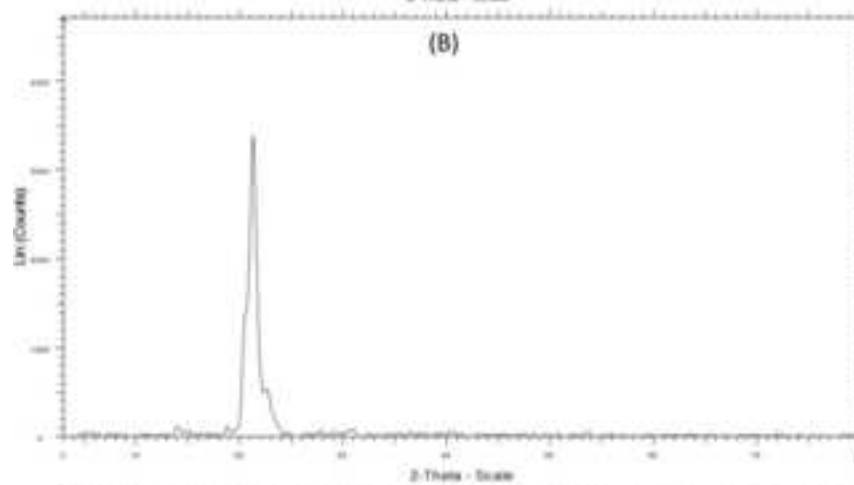
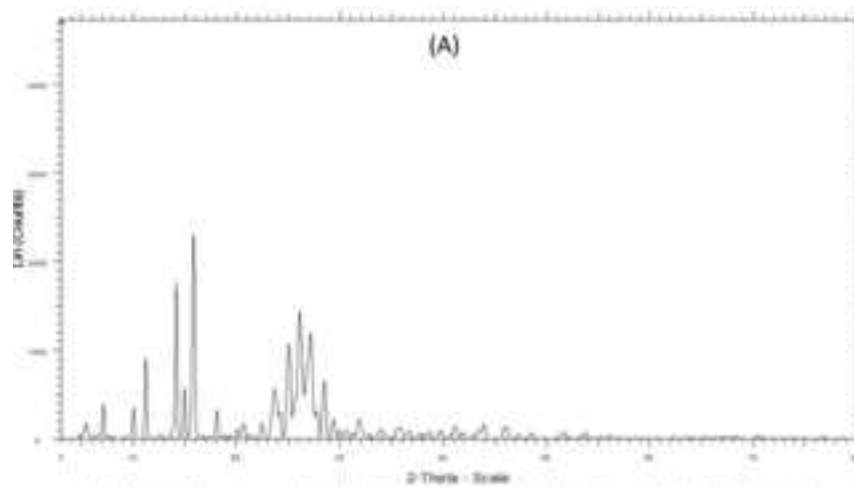
Figure(s)



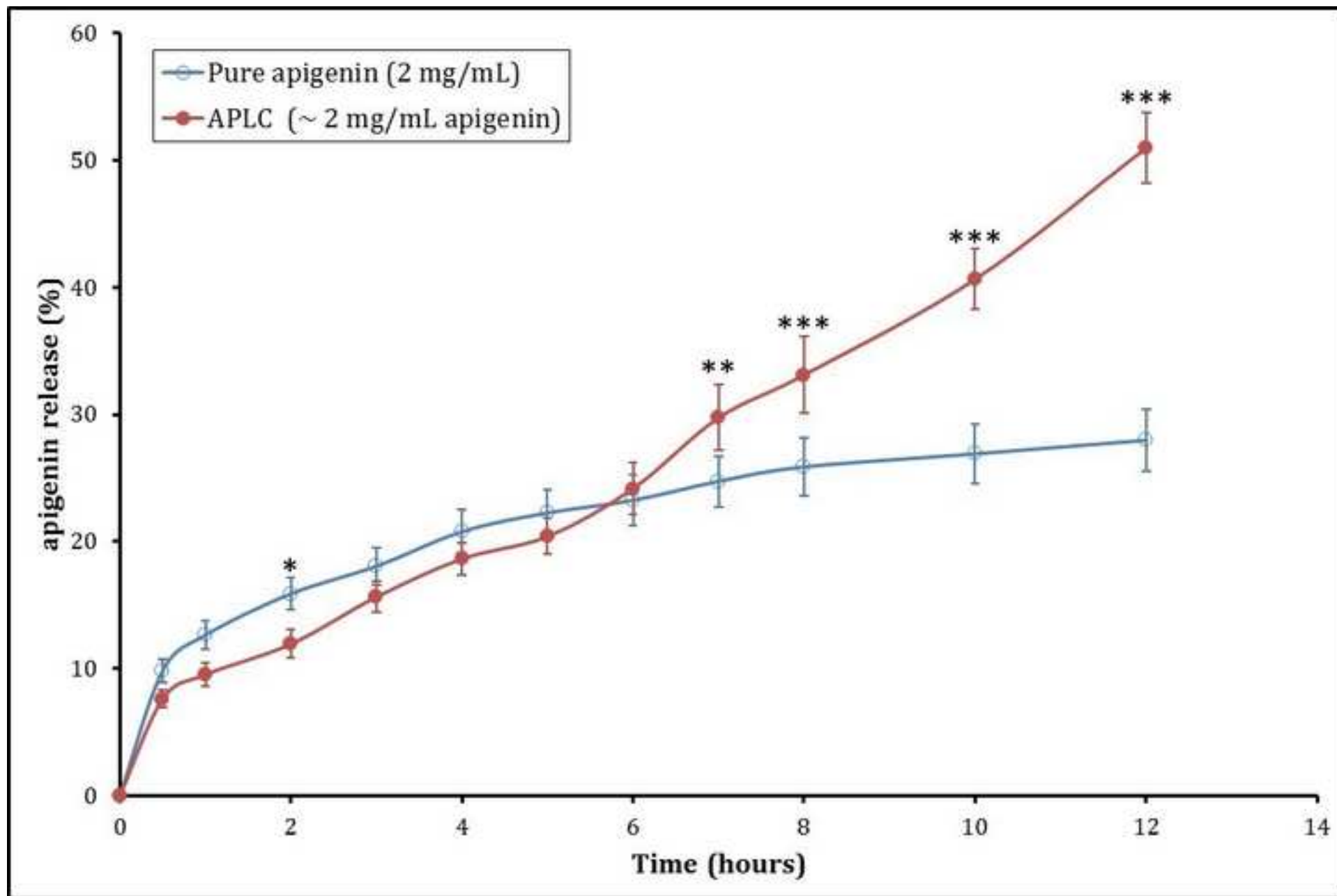
Figure(s)



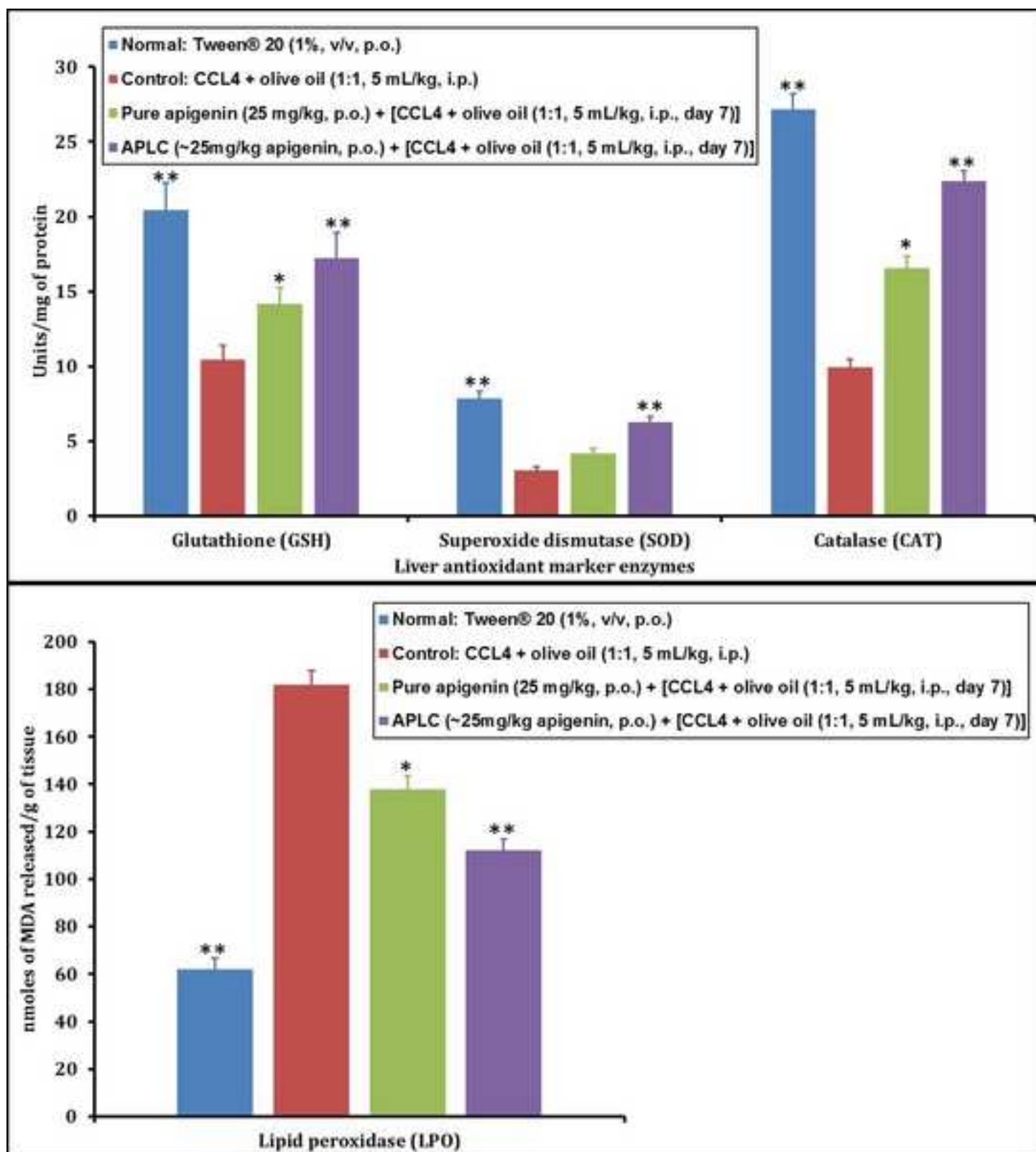
Figure(s)



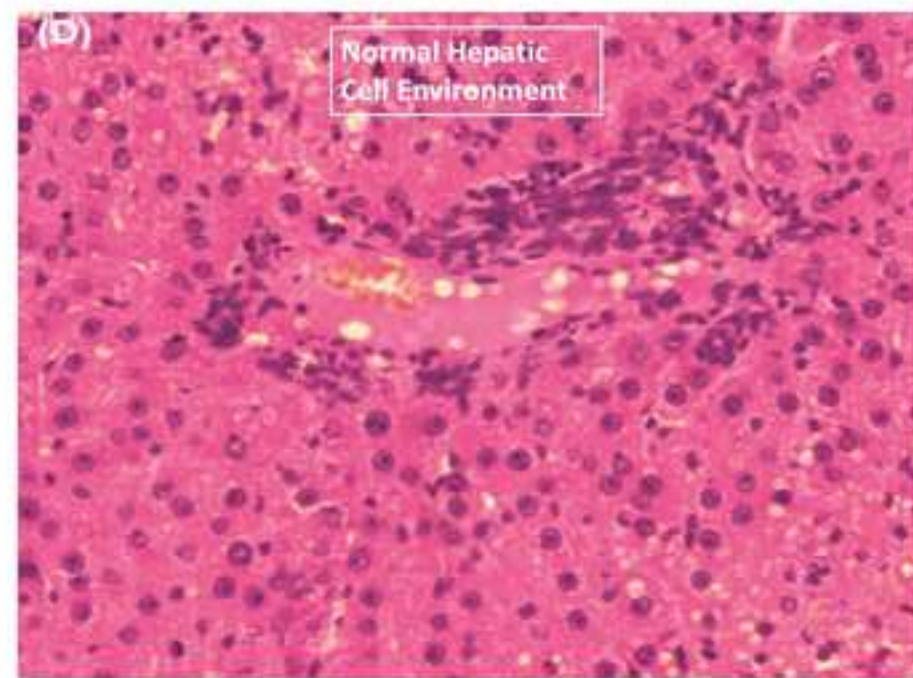
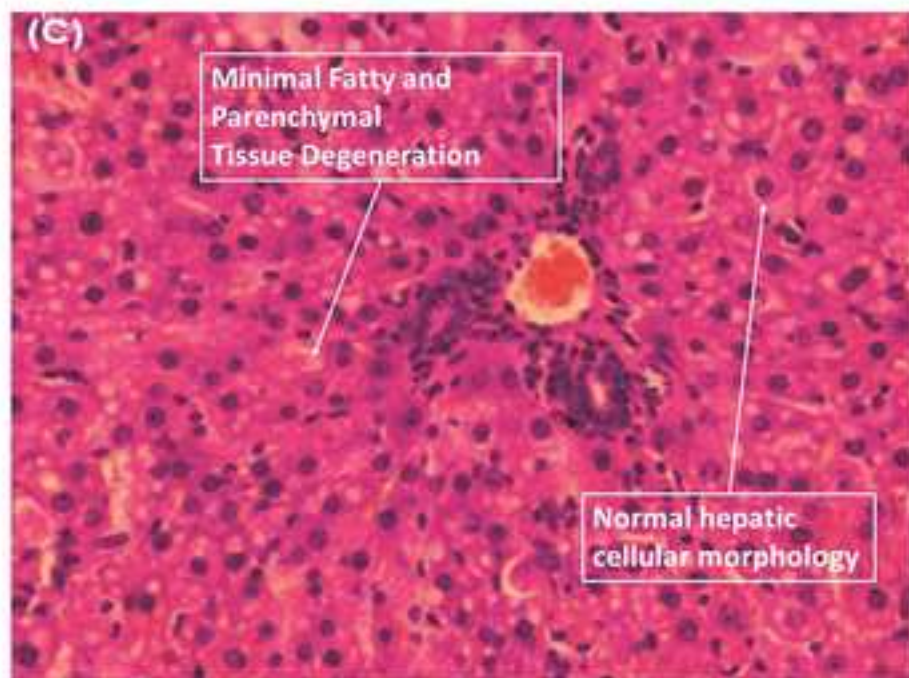
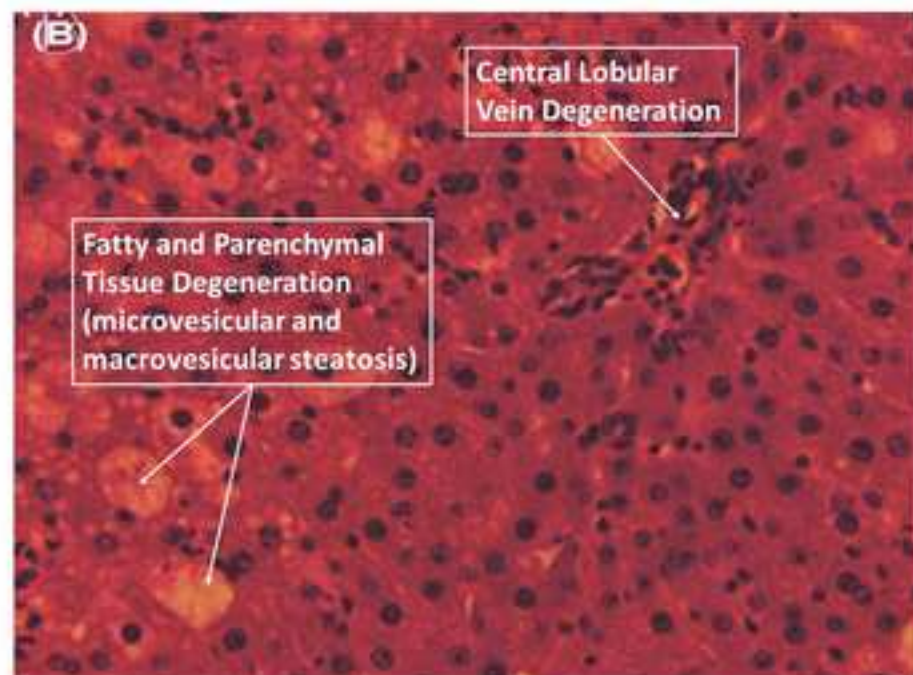
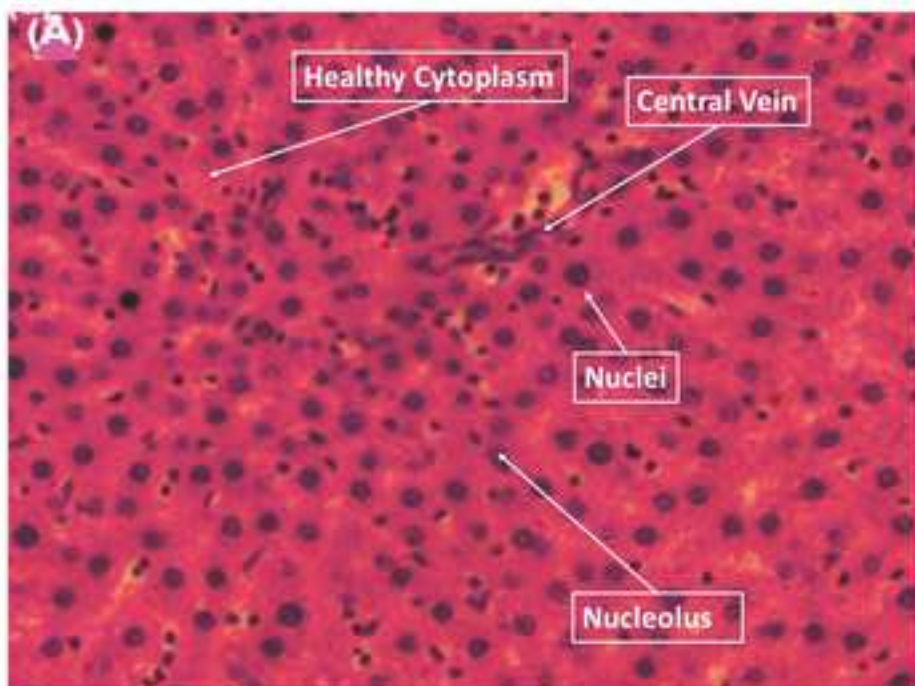
Figure(s)



Figure(s)



Figure(s)



Figure(s)

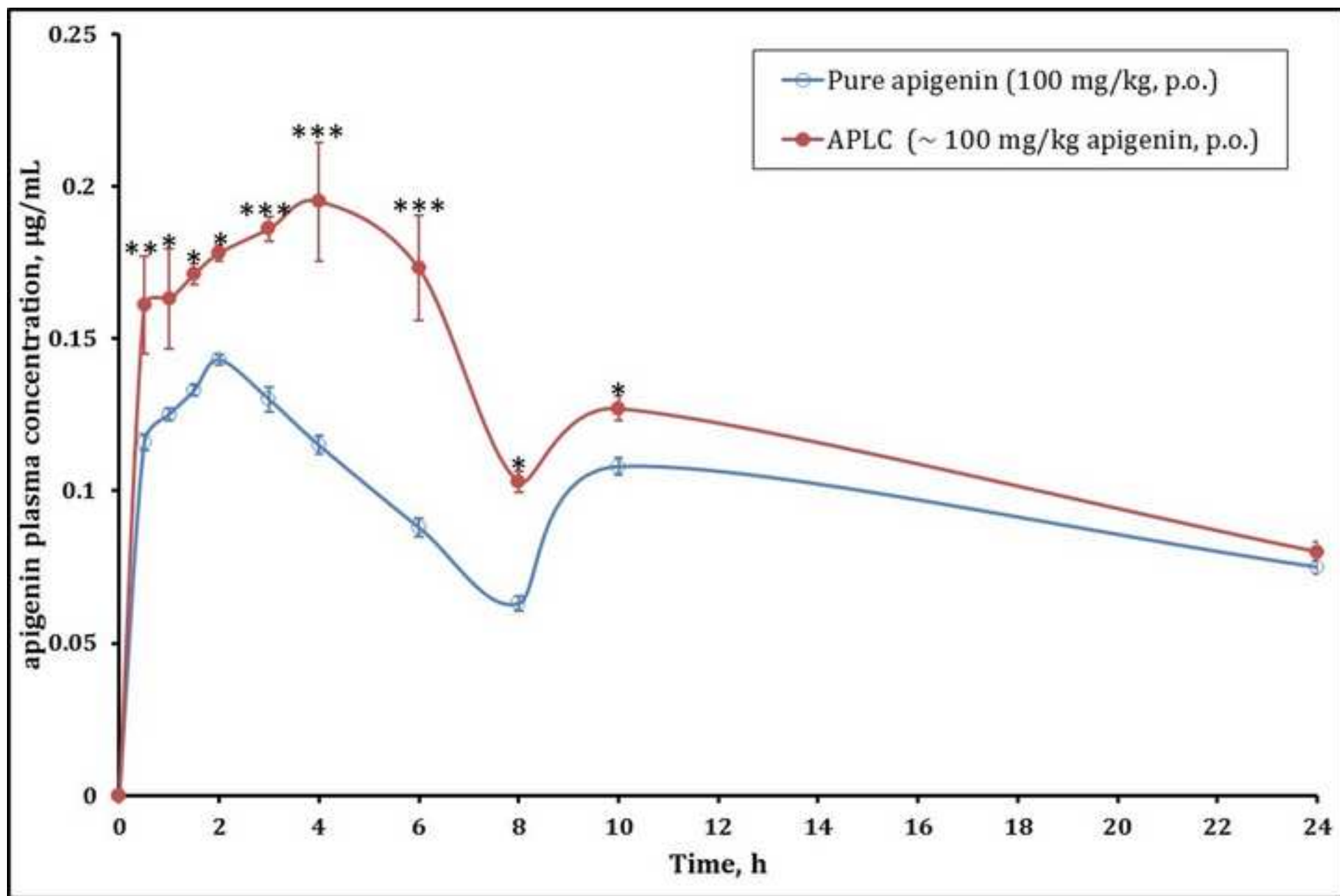


Figure legend

Figure 1. The response surface plot and contour plots of entrapment efficiency (Y , %) as a function of the ratio of apigenin and Phospholipon[®] 90H (X_1 , w:w), and the reaction temperature (X_2 , °C).

Figure 2. DSC thermograms of (A) pure apigenin, (B) Phospholipon[®] 90H, (C) the physical mixture (1:1) of apigenin and Phospholipon[®] 90H, and (D) APLC.

Figure 3. FTIR spectra of (A) pure apigenin, (B) Phospholipon[®] 90H, (C) the physical mixture (1:1) of apigenin and Phospholipon[®] 90H, and (D) APLC.

Figure 4. ¹H-NMR spectra of (A) apigenin, and (B) APLC.

Figure 5. The X-ray diffractograms of (A) pure apigenin, (B) Phospholipon[®] 90H, (C) the physical mixture (1:1) of apigenin and Phospholipon[®] 90H, and (D) APLC.

Figure 6. The in-vitro dissolution profiles of apigenin release from apigenin suspension, and APLC. Values are mean \pm Std. Dev. ($n = 3$). * $p < 0.05$, ** $p < 0.01$, *** $p < 0.001$ (significant with respect to pure apigenin).

Figure 7. Influence of pure apigenin and APLC on rat liver antioxidant marker enzymes, i.e. glutathione reductase (GSH) (nmoles/mg of protein), superoxide dismutase (SOD) (units/mg protein), catalase (CAT) (units/mg protein), and lipid peroxidase (LPO) (nmoles of MDA

released /g tissue). Values are Mean \pm Std. Error of Mean (n = 6). * p < 0.05, ** p < 0.01 (significant with respect to control: CCl₄-only treated groups).

Figure 8. Histopathology micrographs ($\times 400$) of rat livers. (A) Normal: Tween[®] 20 (1%, v/v, p.o.), (B) Control: CCl₄ + olive oil (1:1, 5 mL/kg, i.p.), (C) Pure apigenin (25 mg/kg, p.o.) + [CCl₄ + olive oil (1:1, 5 mL/kg, i.p., day 7)], and (D) APLC (\sim 25 mg/kg apigenin, p.o.) + [CCl₄ + olive oil (1:1, 5 mL/kg, i.p., day 7)].

Figure 9. Mean plasma concentration-time profile after oral administration of pure apigenin (100 mg/kg, p.o.) or APLC (\sim 100 mg/kg apigenin, p.o.). Values are mean \pm Std. Dev. (n = 6). * p < 0.05; ** p < 0.01, and *** p < 0.001 (significant with respect to pure apigenin treated group).

Tables

Table 1. Coded levels and “Real” values for each factor studied

Variables	Levels		
	-1	0	+1
<i>Independent</i>	Real values		
Apigenin : Phospholipid ratio (X_1 , w:w)	1:1	1:2	1:3
Reaction temperature (X_2 , °C)	40	50	60
<i>Dependent</i>			
Extent of apigenin incorporation or Yield (Y , % w/w)			

Table 2. Full factorial design experimental trials along with respectively obtained yield values (% w/w).

Experimental trials	X_1	X_2	Extent of apigenin incorporation, or Yield* (% w/w)
1	0	+1	93.26 ± 0.82
2	0	0	90.28 ± 1.75
3	-1	-1	66.84 ± 1.39
4	+1	+1	89.70 ± 0.72
5	+1	-1	84.88 ± 1.47
6	-1	0	69.31 ± 1.63
7	+1	0	86.05 ± 1.21
8	0	-1	87.43 ± 1.32
9	-1	+1	74.66 ± 0.57

* Values represent mean ± Std. Dev. (n=3)

Table 3. Solubility analysis of pure apigenin, the physical mixture (1:1) of apigenin and Phospholipon[®] 90H (PM), and apigenin- Phospholipon[®] 90H phytosome (APLC).

Sample	Aqueous solubility (µg/mL)*	n-octanol solubility (µg/mL)*
Apigenin	0.62 ± 0.88	603.02 ± 0.72
PM	6.13 ± 1.13	634.77 ± 1.25
APLC	22.80 ± 1.40	680.24 ± 1.21

*Data expressed as mean ± Std. Dev.; n = 3

Table 4. Influence of pure apigenin and APLC on rat liver function markers, Serum Glutamic-Pyruvic Transaminase (SGPT), Serum Glutamic-Oxaloacetic Transaminase (SGOT), Serum Alkaline Phosphatase (SALP), and total bilirubin.

Treatment	SGPT (IU/L) ^a	SGOT (IU/L) ^a	SALP (IU/L) ^a	Total bilirubin (mg/dL)
Normal: Tween [®] 20 (1%, v/v, p.o.)	36.86 ± 1.30**	38.31 ± 1.15**	134.90 ± 2.14**	0.35 ± 0.02**
Control: CCl ₄ + olive oil (1:1, 5 mL/kg, i.p.)	76.94 ± 2.96	90.29 ± 3.47	182.20 ± 4.31	0.90 ± 0.05
Apigenin (25 mg/kg, p.o.) + [CCl ₄ + olive oil (1:1, 5 mL/kg, i.p., day 7)]	63.02 ± 2.45	76.12 ± 1.40*	169.18 ± 2.90*	0.59 ± 0.03*
APLC (~25mg/kg apigenin, p.o.) + [CCl ₄ + olive oil (1:1, 5 mL/kg, i.p., day 7)]	50.90 ± 1.63**	58.07 ± 1.51**	150.25 ± 2.40**	0.46 ± 0.01**

^a - IU/L – International Units/Liter of plasma

All values are Mean ± Std. Error of Mean (*n* = 6)

p* < 0.05, *p* < 0.01 (significant with respect to control group)

Table 5. Estimated pharmacokinetic parameters after oral administration of pure apigenin (100 mg/kg, p.o.) or APLC (~100 mg/kg apigenin, p.o.).

Pharmacokinetic parameters	Treatment	
	Apigenin (100 mg/kg, p.o.)	APLC (~100 mg/kg apigenin, p.o.)
<i>C</i> _{max} (µg ml ⁻¹)	0.14 ± 0.15	0.20 ± 0.25
<i>T</i> _{max} (hours)	2.0 ± 0.23	4.0 ± 0.34
Area under concentration-time curve (<i>AUC</i> _{0-t}) (µg ml ⁻¹ h)	0.84 ± 0.42	1.31 ± 0.46
Area under concentration-time curve (<i>AUC</i> _{0-∞}) (µg ml ⁻¹ h)	1.27 ± 0.28	1.95 ± 0.65
Elimination half-life (<i>t</i> _{1/2el}) (h)	4.80 ± 0.33	4.34 ± 0.52
Elimination rate constant (<i>K</i> _{el}) (h ⁻¹)	0.16 ± 0.04	0.14 ± 0.03
Clearance (<i>cl/F</i>) [(mg)/(µgml ⁻¹ h ⁻¹)]	78.6 ± 0.45	51.18 ± 0.37
Volume of distribution (<i>V</i> _{z/F}) [(mg)/(µgml ⁻¹ h ⁻¹)]	544.15 ± 0.31	320.72 ± 0.25

All values are Mean ± Std. Error of Mean (*n* = 6)